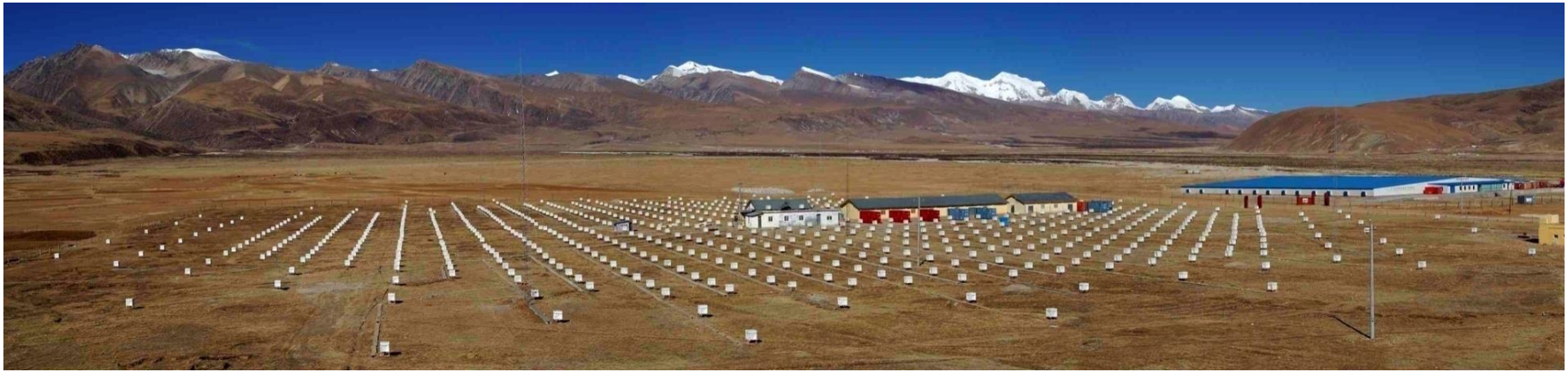

Searching for Galactic PeVatrons with the Tibet ASγ Experiment

Kazumasa KAWATA (ICRR, University of Tokyo)

For the Tibet ASγ Collaboration

Tibet ASγ Collaboration

M. Amenomori[1], S. Asano[2], Y. W. Bao[3], X. J. Bi[4], D. Chen[5], T. L. Chen[6], W. Y. Chen[4], Xu Chen[4,5], Y. Chen[3], Cirennima[6], S. W. Cui[7], Danzengluobu[6], L. K. Ding[4], J. H. Fang[4,8], K. Fang[4], C. F. Feng[9], Zhaoyang Feng[4], Z. Y. Feng[10], Qi Gao[6], A. Gomi[11], Q. B. Gou[4], Y. Q. Guo[4], Y. Y. Guo[4], Y. Hayashi[2], H. H. He[4], Z. T. He[7], K. Hibino[12], N. Hotta[13], Haibing Hu[6], H. B. Hu[4], K. Y. Hu[4,8], J. Huang[4], H. Y. Jia[10], L. Jiang[4], P. Jiang[5], H. B. Jin[5], K. Kasahara[14], Y. Katayose[11], C. Kato[2], S. Kato[15], I. Kawahara[11], T. Kawashima[15], K. Kawata[15], M. Kozai[16], D. Kurashige[11], Labaciren[6], G. M. Le[17], A. F. Li[4,9,18], H. J. Li[6], W. J. Li[4,10], Y. Li[5], Y. H. Lin[4,8], B. Liu[19], C. Liu[4], J. S. Liu[4], L. Y. Liu[5], M. Y. Liu[6], W. Liu[4], X. L. Liu[5], Y.-Q. Lou[20,21,22], H. Lu[4], X. R. Meng[6], Y. Meng[4,8], K. Munakata[2], K. Nagaya[11], Y. Nakamura[15], Y. Nakazawa[23], H. Nanjo[1], C. C. Ning[6], M. Nishizawa[24], R. Noguchi[11], M. Ohnishi[15], S. Okukawa[11], S. Ozawa[25], L. Qian[5], X. Qian[5], X. L. Qian[26], X. B. Qu[27], T. Saito[28], Y. Sakakibara[11], M. Sakata[29], T. Sako[15], T. K. Sako[15], T. Sasaki[12], J. Shao[4,9], M. Shibata[11], A. Shiomi[23], H. Sugimoto[30], W. Takano[12], M. Takita[15], Y. H. Tan[4], N. Tateyama[12], S. Torii[31], H. Tsuchiya[32], S. Udo[12], H. Wang[4], Y. P. Wang[6], Wangdui[6], H. R. Wu[4], Q. Wu[6], J. L. Xu[5], L. Xue[9], Z. Yang[4], Y. Q. Yao[5], J. Yin[5], Y. Yokoe[15], N. P. Yu[5], A. F. Yuan[6], L. M. Zhai[5], C. P. Zhang[5], H. M. Zhang[4], J. L. Zhang[4], X. Zhang[3], X. Y. Zhang[9], Y. Zhang[4], Yi Zhang[33], Ying Zhang[4], S. P. Zhao[4], Zhaxisangzhu[6], X. X. Zhou[10] and Y. H. Zou[4,8]

1 Department of Physics, Hirosaki Univ., Japan.
2 Department of Physics, Shinshu Univ., Japan.
3 School of Astronomy and Space Science, Nanjing Univ., China.
4 Key Laboratory of Particle Astrophysics, Institute of High Energy Physics, CAS, China.
5 National Astronomical Observatories, CAS, China.
6 Department of Mathematics and Physics, Tibet Univ., China.
7 Department of Physics, Hebei Normal Univ., China.
8 Univ. of Chinese Academy of Sciences, China.
9 Institute of Frontier and Interdisciplinary Science and Key Laboratory of Particle Physics and Particle Irradiation (MOE), Shandong Univ., China.
10 Institute of Modern Physics, SouthWest Jiaotong Univ., China.
11 Faculty of Engineering, Yokohama National Univ., Japan.
12 Faculty of Engineering, Kanagawa Univ., Japan.
13 Faculty of Education, Utsunomiya Univ., Japan.
14 Faculty of Systems Engineering, Shibaura Institute of Technology, Japan.
15 Institute for Cosmic Ray Research, Univ. of Tokyo, Japan.
16 Polar Environment Data Science Center, Joint Support-Center for Data Science Research, Research Organization of Information and Systems, Japan.
17 National Center for Space Weather, China Meteorological Administration, China.
18 School of Information Science and Engineering, Shandong Agriculture Univ., China.
19 Department of Astronomy, School of Physical Sciences, Univ. of Science and Technology of China, China.
20 Department of Physics and Tsinghua Centre for Astrophysics (THCA), Tsinghua Univ., China.
21 Tsinghua Univ.-National Astronomical Observatories of China (NAOC) Joint Research Center for Astrophysics, Tsinghua Univ., China.
22 Department of Astronomy, Tsinghua Univ., China.
23 College of Industrial Technology, Nihon Univ., Japan.
24 National Institute of Informatics, Japan.
25 National Institute of Information and Communications Technology, Japan.
26 Department of Mechanical and Electrical Engineering, Shangdong Management Univ., China.
27 College of Science, China Univ. of Petroleum, China.
28 Tokyo Metropolitan College of Industrial Technology, Japan.
29 Department of Physics, Konan Univ., Japan.
30 Shonan Institute of Technology, Japan.
31 Research Institute for Science and Engineering, Waseda Univ., Japan.
32 Japan Atomic Energy Agency, TJapan.
33 Key Laboratory of Dark Matter and Space Astronomy, Purple Mountain Observatory, CAS, China.

Outline

1. Introduction
2. Tibet ASγ Experiment
3. Galactic Diffuse Gamma Rays
4. PeVatron Candidates
5. Summary

Introduction

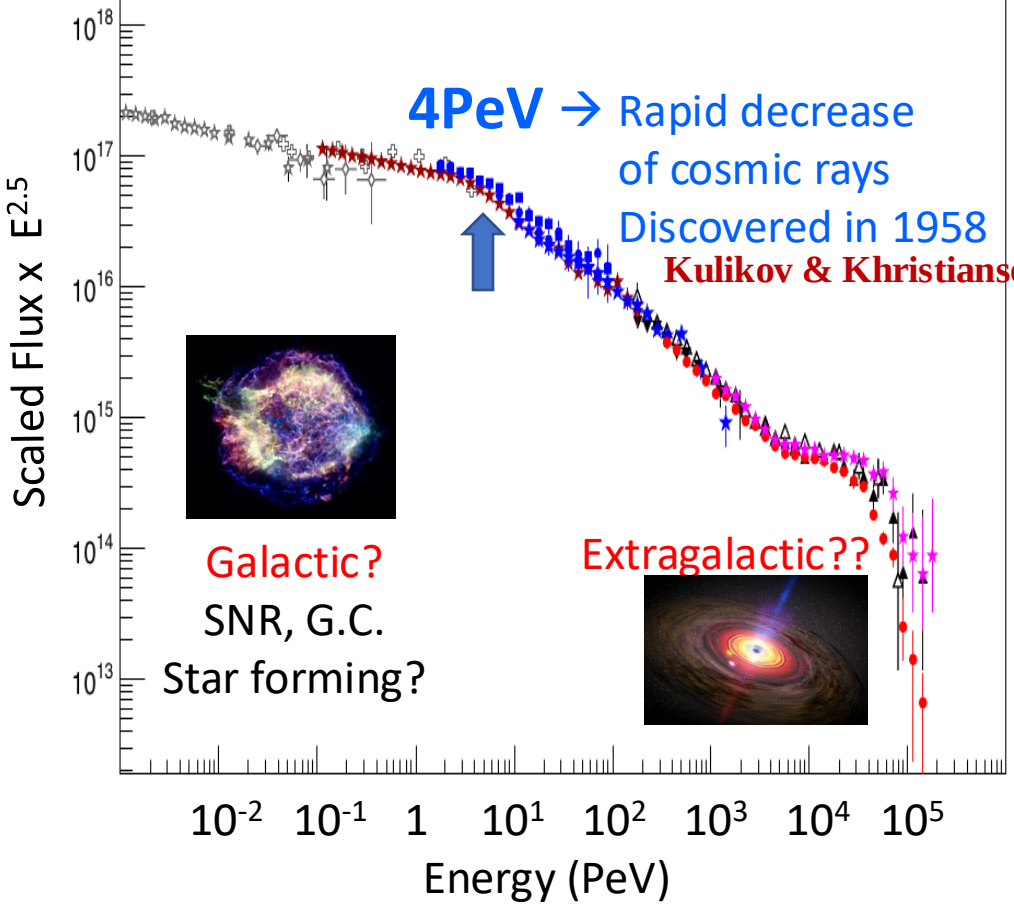

- Wide energy range
- Main component is proton
- Rate decreases to 1/100 when energy is 10 times higher

As an open question,
Did/Do "PeVatrons" really exist in our Galaxy?

PeVatron: Cosmic super-accelerators can accelerate to Peta electron volt

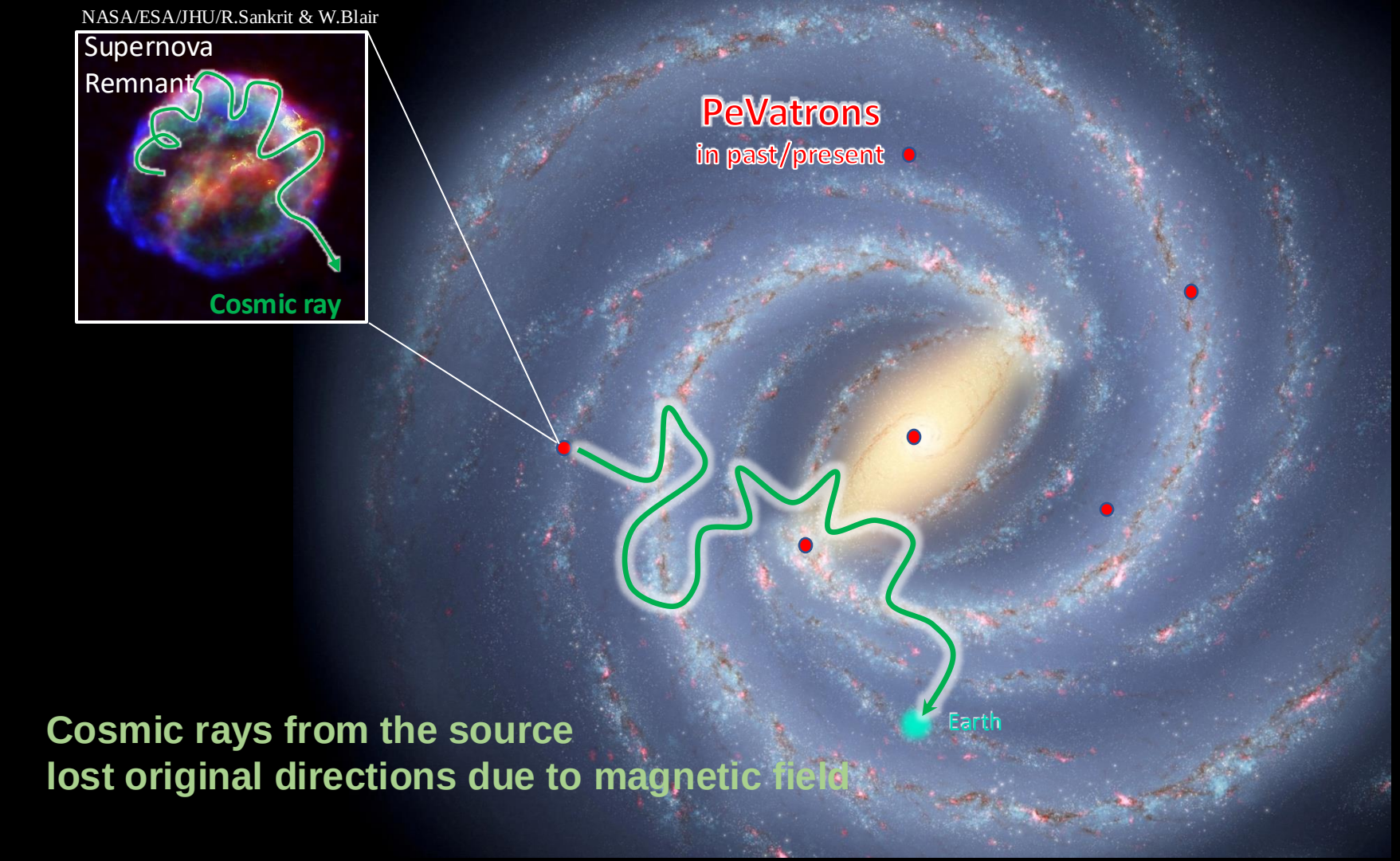

Cosmic rays from the source lost original directions due to magnetic field

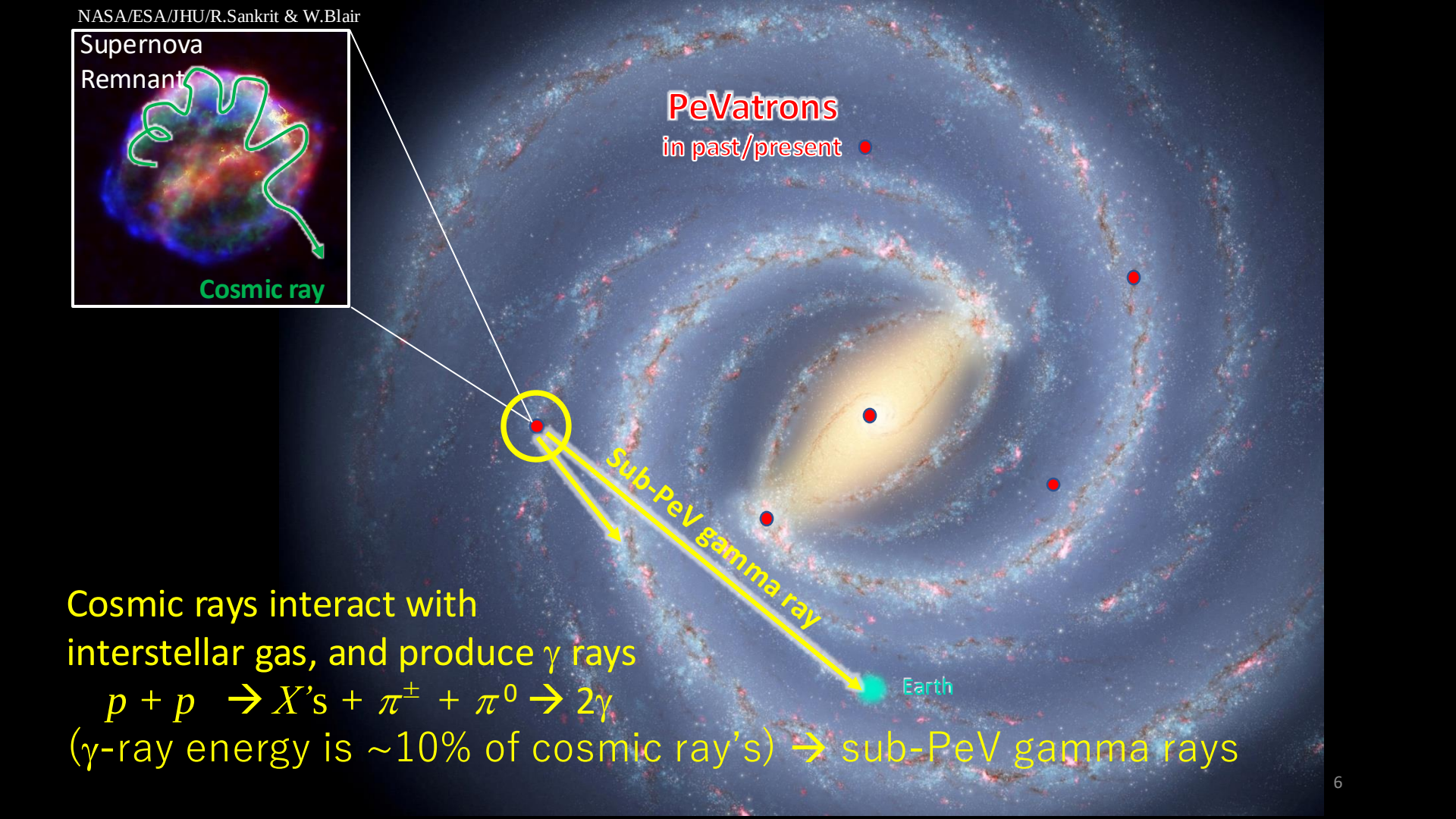

Cosmic rays interact with interstellar gas, and produce γ rays

$p + p \rightarrow X\text{'s} + \pi^{\pm} + \pi^{0} \rightarrow 2\gamma$

(γ-ray energy is ~10% of cosmic ray's) → sub-PeV gamma rays

Tibet Air Shower Array

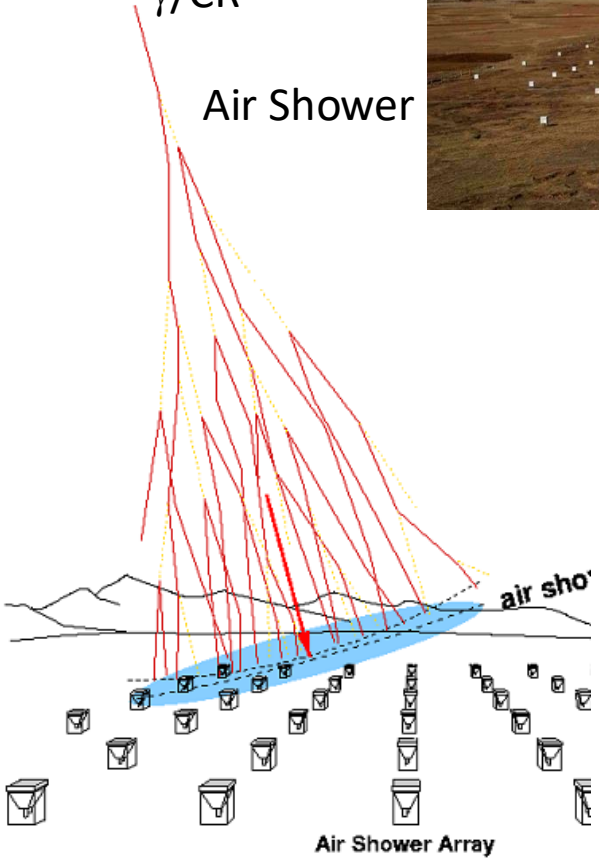

- Site: Tibet (90.522°E, 30.102°N) 4,300 m a.s.l.

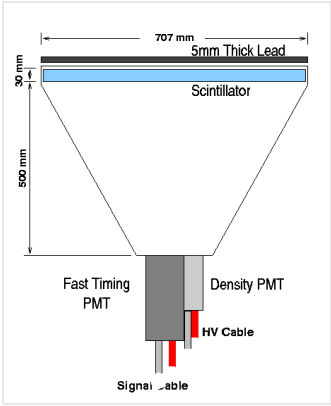

Present Performance

✓	# of detectors	0.5 m^2 x 597
✓	Covering area	~65,700 m^2
✓	Angular resolution	~0.5° @10TeV γ
		~0.2° @100TeV γ
✓	Energy resolution	~40%@10TeV γ
		~20%@100TeV γ

→Observation of secondary (mainly $e^{+/-}$,γ) in AS
Primary energy : 2nd particle densities
Primary direction : 2nd relative timings

Air Shower Reconstruction

Gamma-ray candidate event

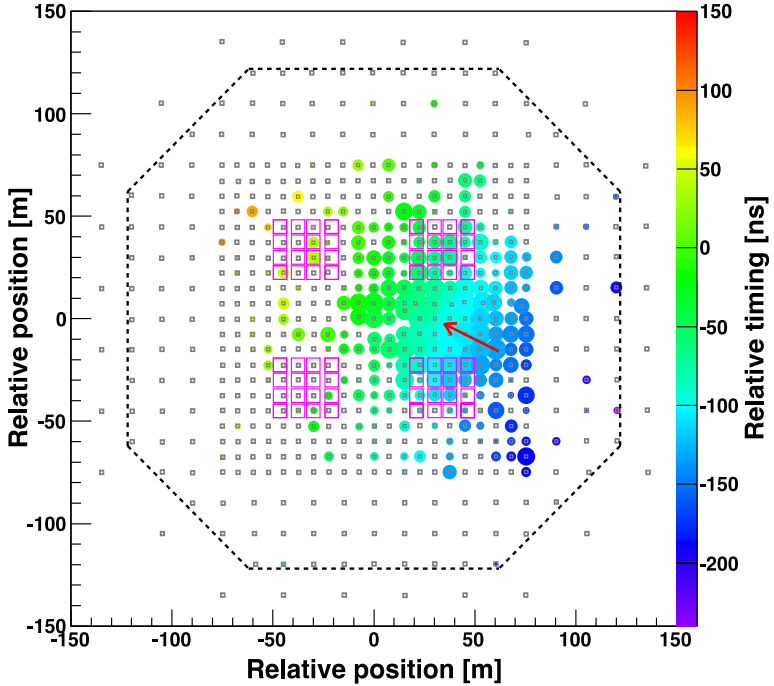

circle size ∝ log(# of detected particles)
circle color ∝ relative timing [ns]

Amenomori +, PRL ***123****, 051101 (2019)*

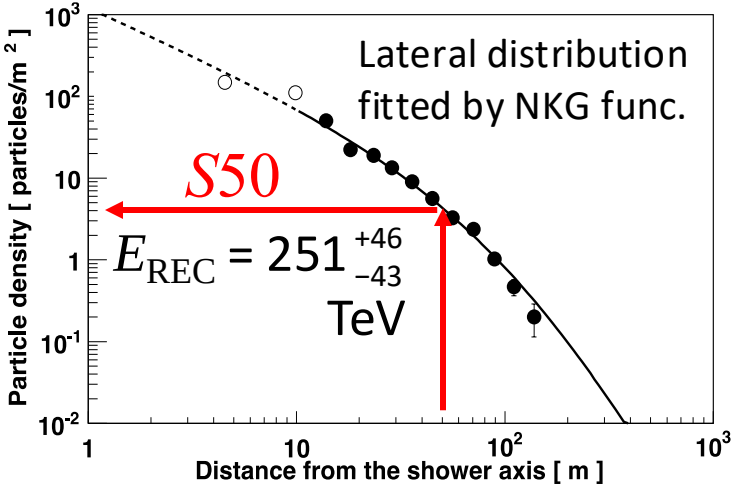

S50 improves E resolutions (10 - 1000 TeV)
→ ~40%@10 TeV , ~20%@100 TeV

Kawata+, Experimental Astronomy ***44****, 1 (2017)*

Underground WC Muon Detectors

- ✓ 4 pools, 16 units / pool
- ✓ 54 m^2 in area $\times$1.5m in depth / unit
- ✓ 20”ΦPMT (HAMAMATSU R3600)
- ✓ Concrete pools + white Tyvek sheets
- ✓ 2.4m soil overburden (~515g/cm^2 ~9X_0)

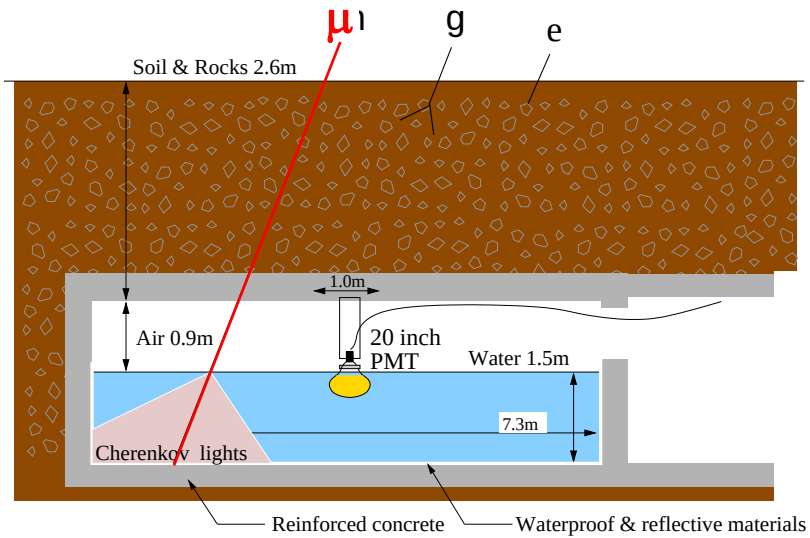

Measurement of # of μ in AS → γ／CR discrimination
DATA: February 2014 - May 2017 Live time: 719 days

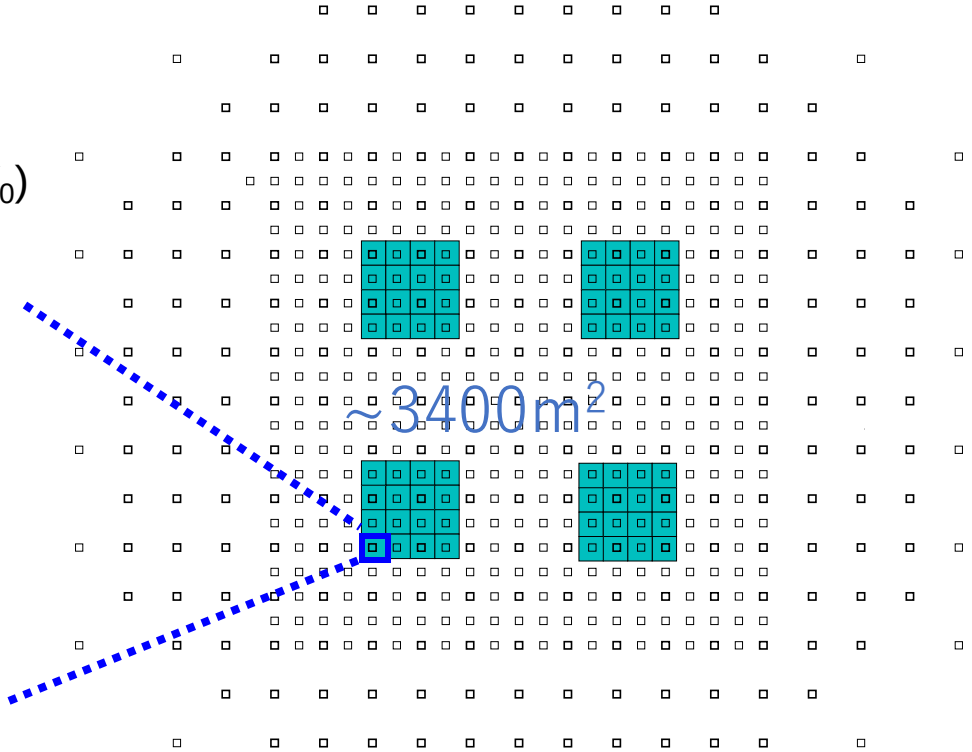

→Succeeded in rejecting by >99.9% CR events

Basic idea: Sako et al., Astropart. Phys., 32, 177 (2009)

Gamma-Ray Selection

γ-ray → poor muons

Muons can penetrate underground

200TeV γ-ray

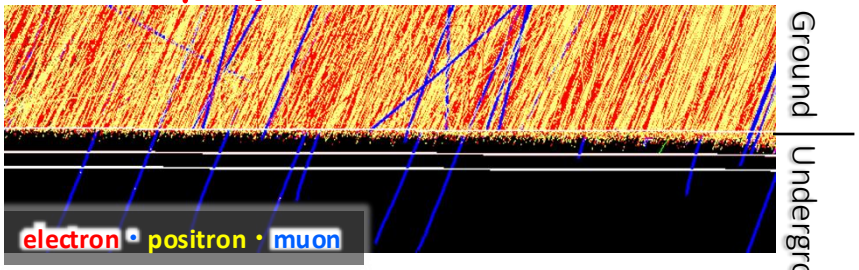

200TeV Cosmic ray (Noise)

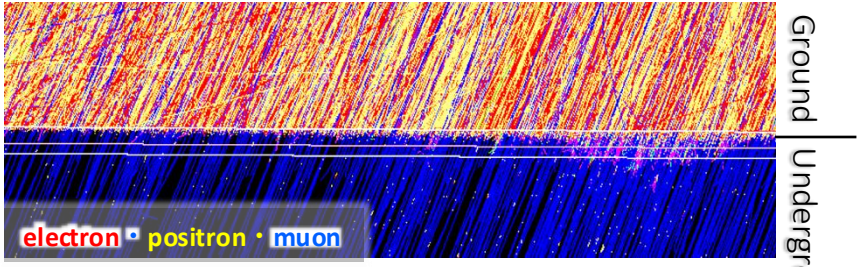

→ Underground muon detectors

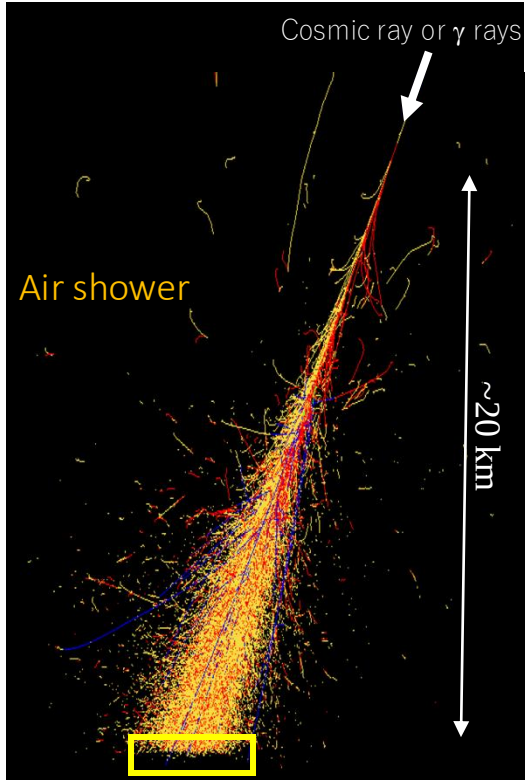

Simulated by COSMOS

Enlarged view

Muon Cut Condition (Standard)

Standard muon cut : $\Sigma N\mu < 2.1 \times 10^{-3}\ \Sigma\rho^{1.2}$ → Optimized for the gamma-ray point-like source

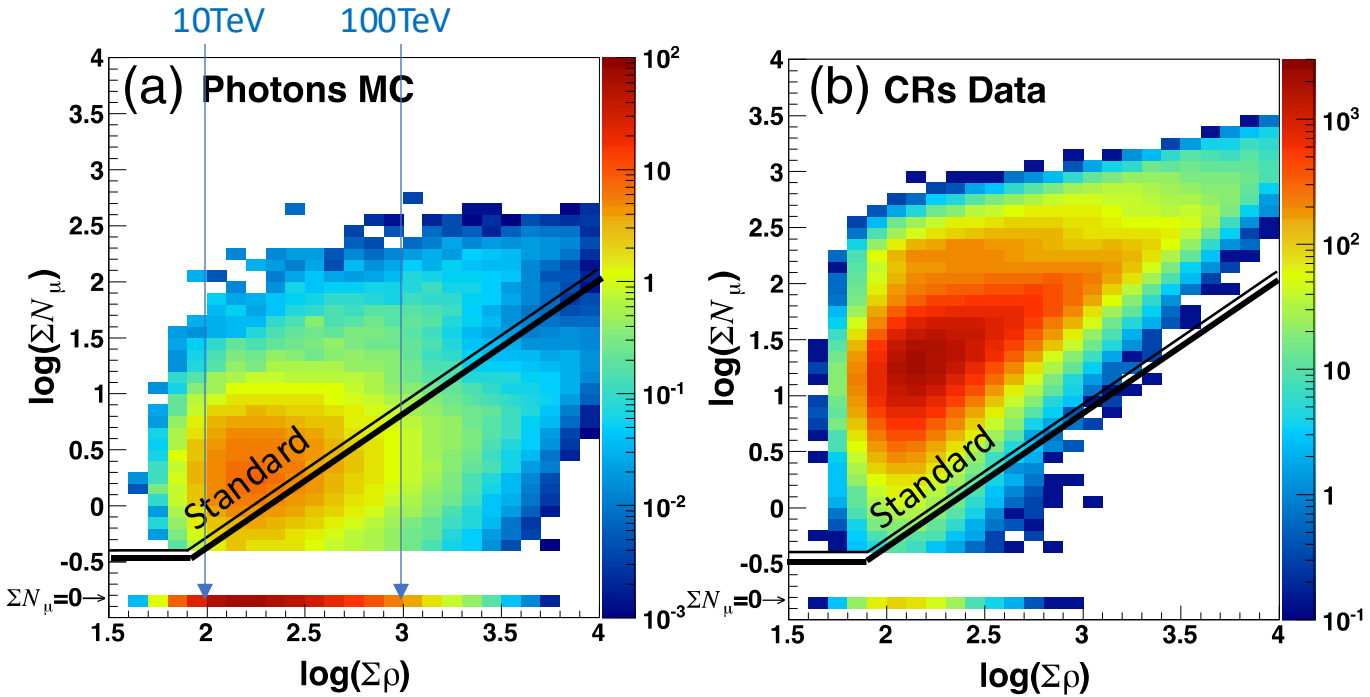

Gamma Survival ratio : ~90% by MC sim (>100TeV) CR Survival ratio : ~10^{-3} (>100TeV)

Muon Number Distribution (Crab >100 TeV)

Data/MC Comparison

$$R\mu = \frac{\text{Observed \# of muons}}{\text{\# of muons at the cut value}}$$

$R\mu < 1$ → γ-like

$R\mu > 1$ → CR-like

Gamma Survival ratio :
90% by MC sim (>100TeV)

CR Survival ratio :
~0.1%(>100TeV)

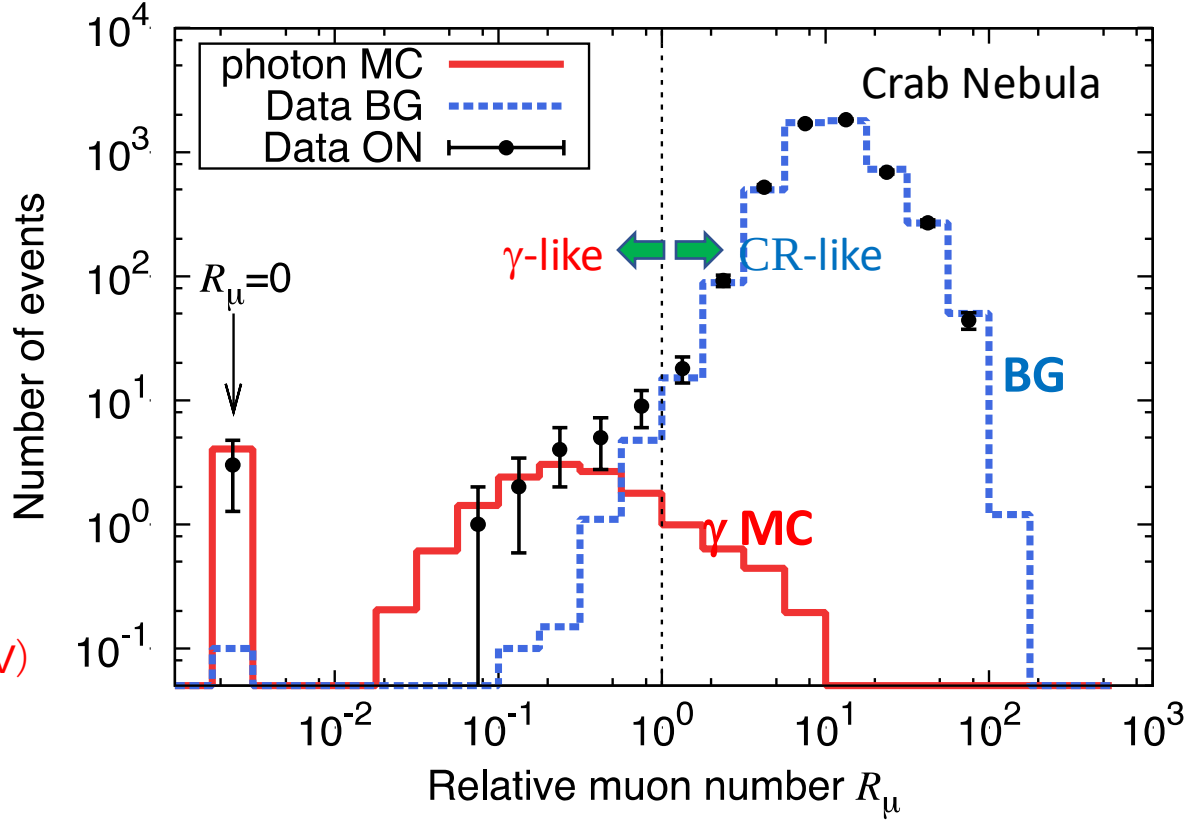

UHE γ-rays from the Crab Nebula (2019)

Amenomori et al., PRL 123, 051101 (2019)

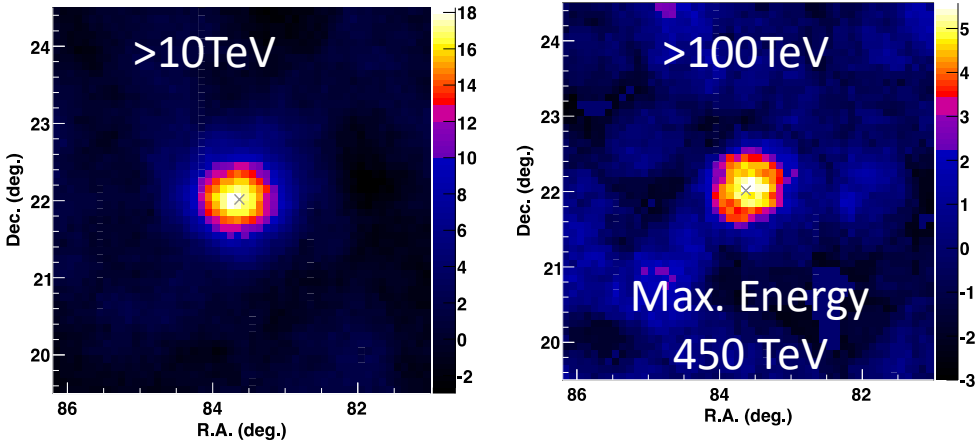

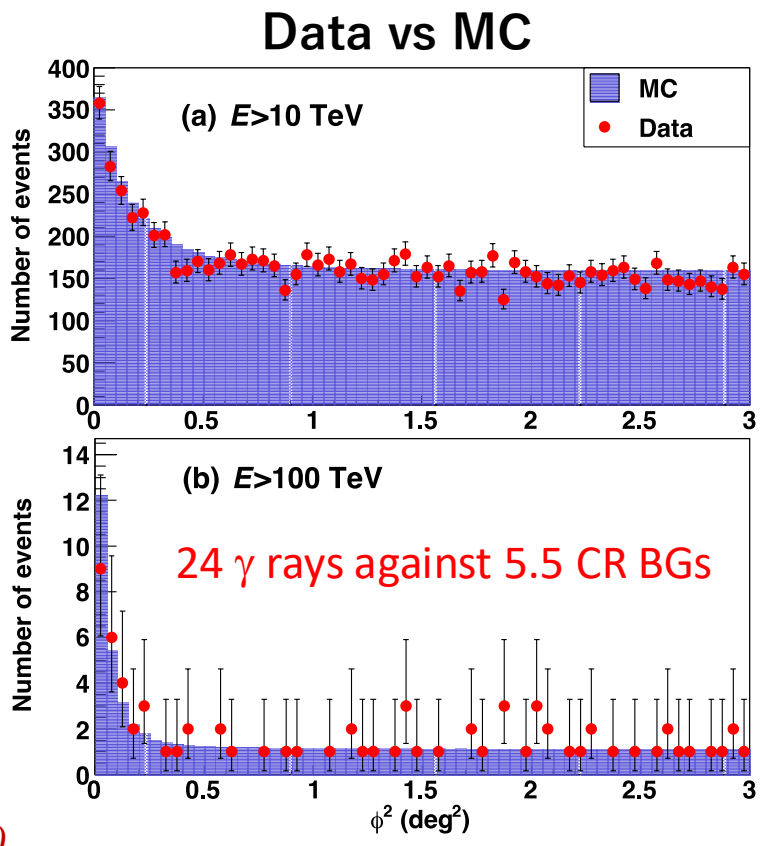

First Detection of Sub-PeV γ (5.6σ)

Other detected sources in 100 TeV region

- ✓ G106.3+2.7 *Amenomori et al., Nat. Astron, 5, 460 (2021)*
- ✓ Cygnus OB1 *Amenomori et al., PRL, 127, 031102 (2021)*
- ✓ Cygnus OB2
- ✓ HESS J1843-033 *Amenomori et al., ApJ, 932, 120 (2022)*
- ✓ HESS J1849-000 *Amenomori et al, ApJ, 954, 200 (2023)*

UHE γ-rays from the Crab Nebula (2019)

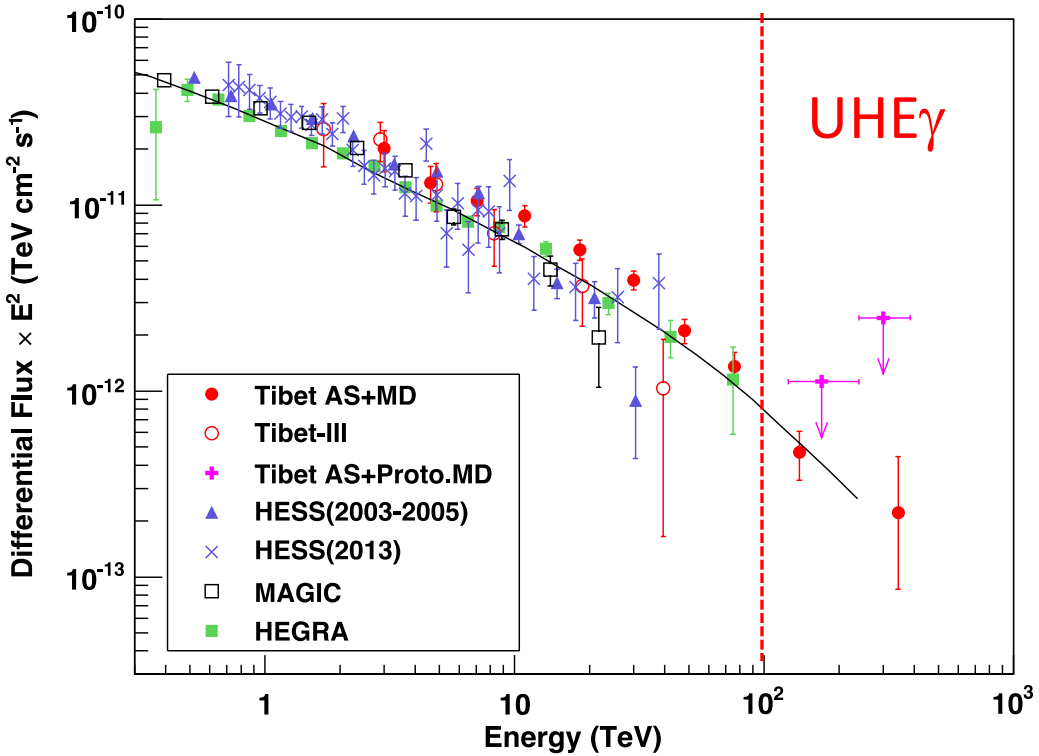

*Amenomori+, PRL, **123**, 051101, (2019)*

No energy cutoff beyond 100 TeV

Thick curve：
inverse Compton model
normalized to HEGRA data
Aharonian+, ApJ, 614, 897 (2004)

Muon Cut Condition (Tight) for Diffuse γ

Tight muon cut : $\Sigma N\mu < 2.1 \times 10^{-4} \Sigma\rho^{1.2}$ → One order magnitude tighter than the Crab analysis

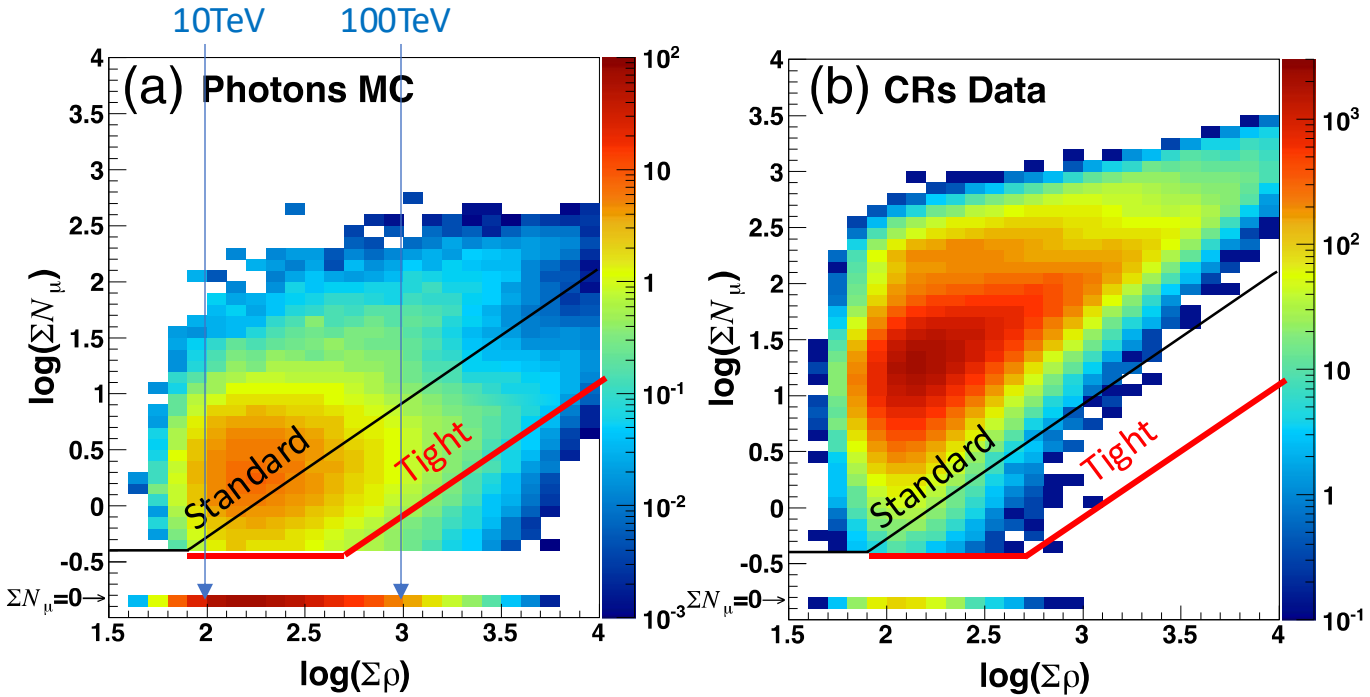

Gamma Survival ratio : ~30% by MC sim (>398TeV) CR Survival ratio : ~10^{-6} (>398TeV=$10^{2.6}$TeV)

γ-ray-like event Distribution

Amenomori et al., PRL 126, 141101 (2021)

Gamma-ray-like events
after the tight muon cut
in the equatorial coordinates

Blue points:
Experimental data
Red plus marks:
known Galactic TeV sources

>398 TeV ($10^{2.6}$ TeV)
38 events in our FoV
23 events in $|b| < 10^{o}$
16 events in $|b| < 5^{o}$

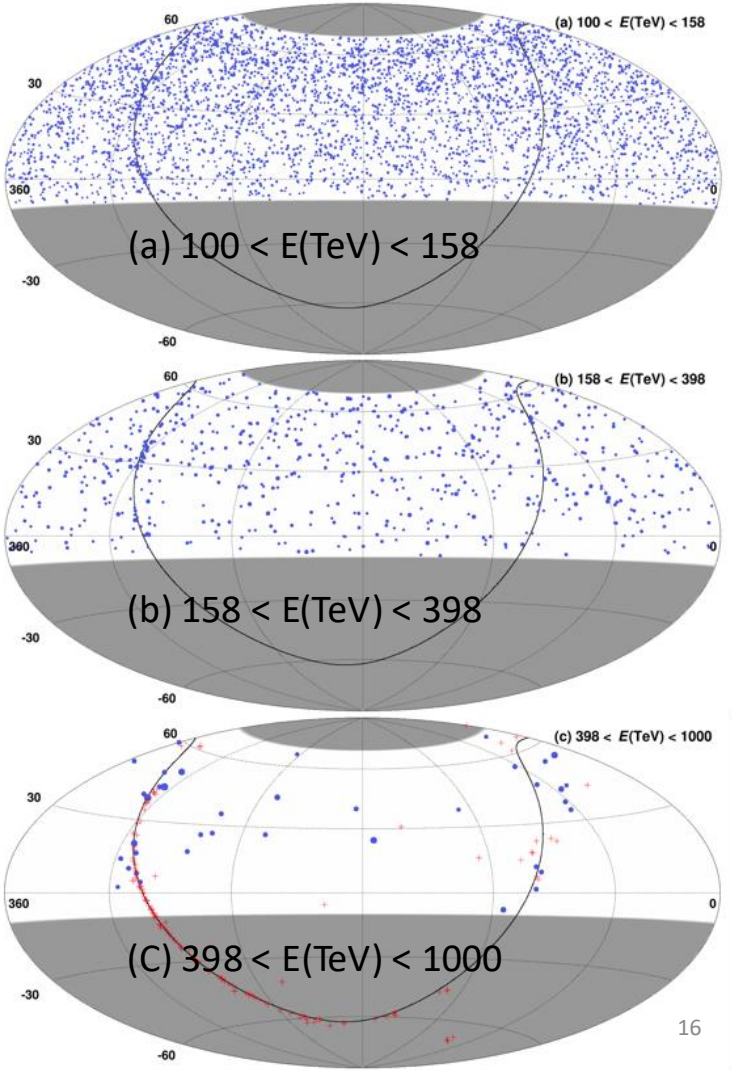

Latitude Profile

6.6σ

Amenomori et al., PRL 126, 141101 (2021)

Red points:
experimental data across
our FoV ($22^o < l < 225^o$)
including source contribution

5.1σ

Gray shade histogram:
Model by Lipari and Vernetto

Lipari & Vernetto, PRD 98, 043003 (2018)

5.9σ

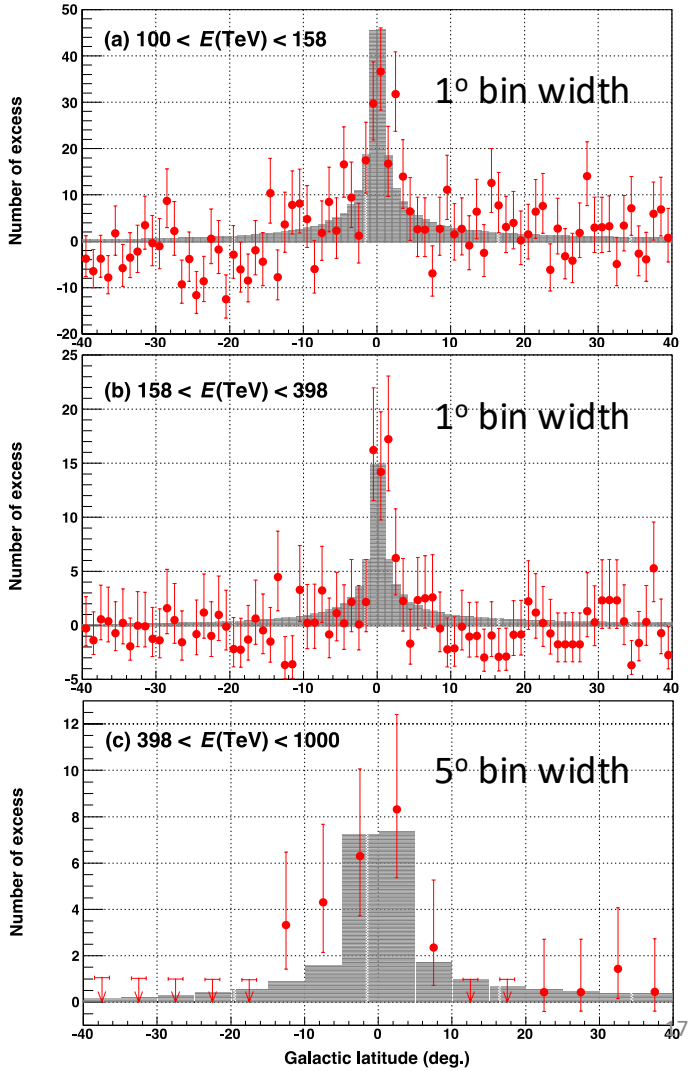

Correlation with known TeV Sources

Correlation between UHE γ-rays above 398 TeV and 60 galactic sources from TeVCat catalog including UNID, PWN , Shell, Binary, SNR…, excluding GRB, HBL, IBL, LBL, BL Lac, AGN, Blazar, FSRQ, FRI, Starburst)

- ✓ No excess around known TeV sources
- ✓ Event distribution is consistent with diffuse model

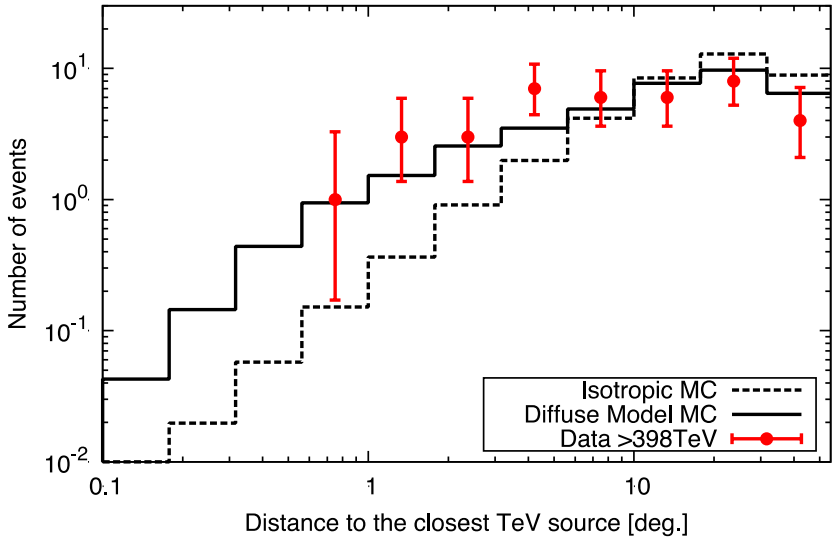

- ✓ High-energy $e^{+/-}$ lose their energy quickly.
- ✓ Cosmic-ray protons can escape farther from the source.

Strong evidence for sub-PeV γ rays induced by cosmic rays

Energy Spectrum of UHE Diffuse γ Rays

Amenomori et al., PRL 126, 141101 (2021)

After excluding the contribution from the known TeV sources (within 0.5 degrees) listed in the TeV source catalog

The measured fluxes are overall consistent with Lipari's diffuse gamma model assuming the hadronic cosmic ray origin.

CR + ISM → X's + π^0 ... → 2γ

Lipari & Vernetto, PRD 98, 043003 (2018)

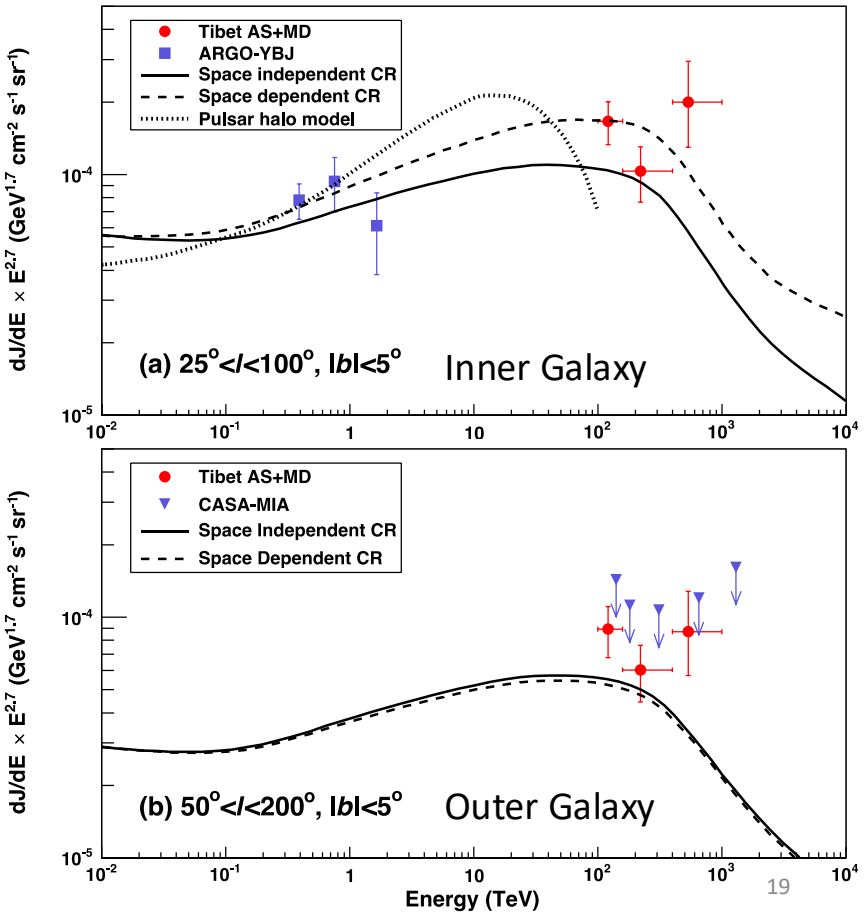

PeVatron Candidate: Cygnus Cocoon

Abeysekara et al., Nature Astronomy (2021)

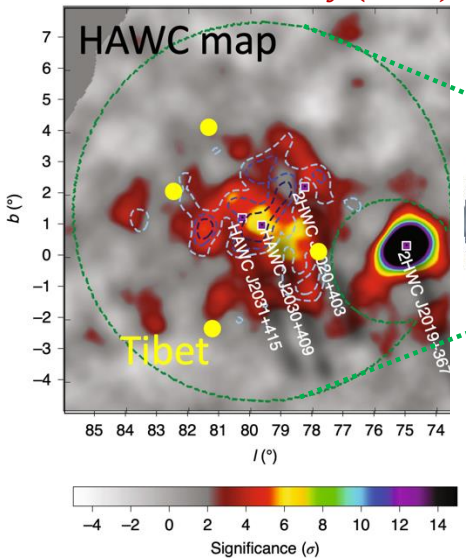

Amenomori et al., PRL 126, 141101 (2021)

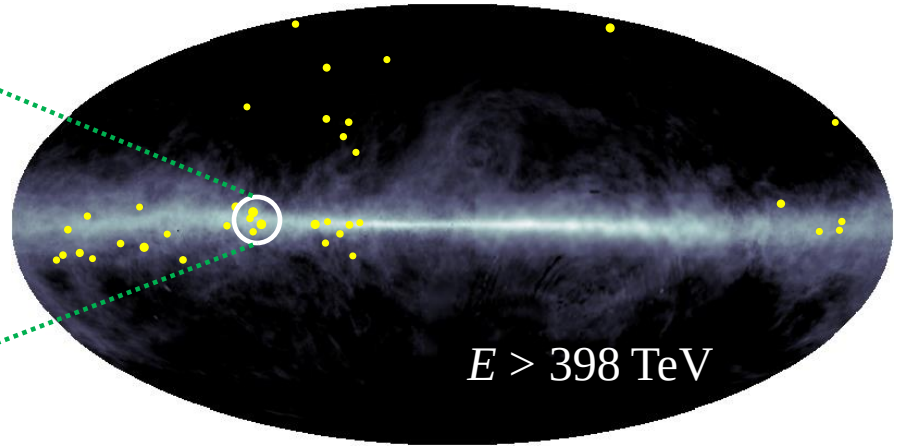

Galactic Coordinates

Fang & Murase, ApJ, 919, 93 (2021)

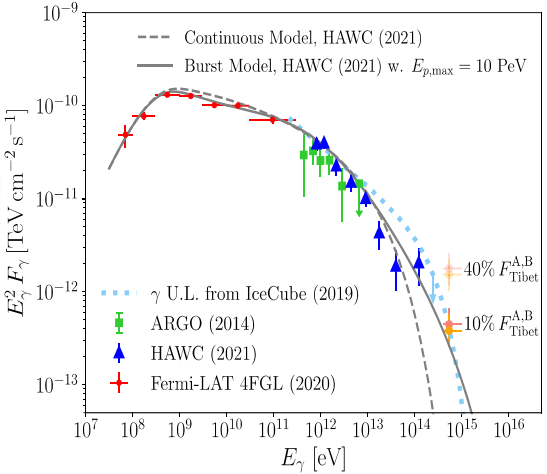

4 events above 398 TeV detected within 4º-radius-circle from the Cygnus cocoon which is claimed as an extended source by the ARGO-YBJ/HAWC/LHAASO and also proposed as a candidate of the PeVatrons.

LHAASO Diffuse Gamma Rays

Z. Cao et al. (LHAASO Collob.) PRL, 131, 151001 (2023)

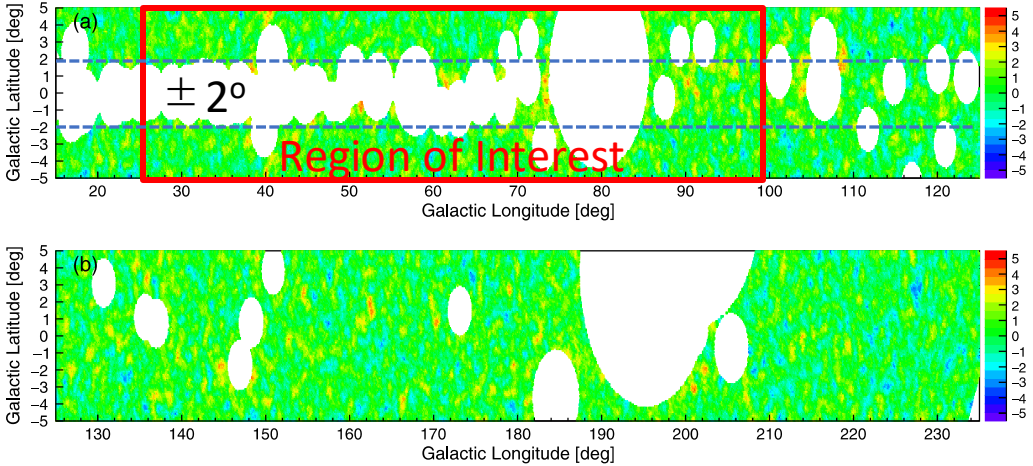

FIG. 1. The significance maps in Galactic coordinate of the inner Galaxy region [panel (a)] and outer Galaxy region [panel (b)] above 25 TeV after masking the resolved KM2A and TeVCat sources.

LHAASO flux is a few times lower than Tibet flux,
LHAASO conservatively masks most of region $l \pm 2^o$.
→ This discrepancy can be explained assuming diffuse gamma ray latitude profile.

K. Fang & K. Murase, ApJ, 957, L6 (2023)

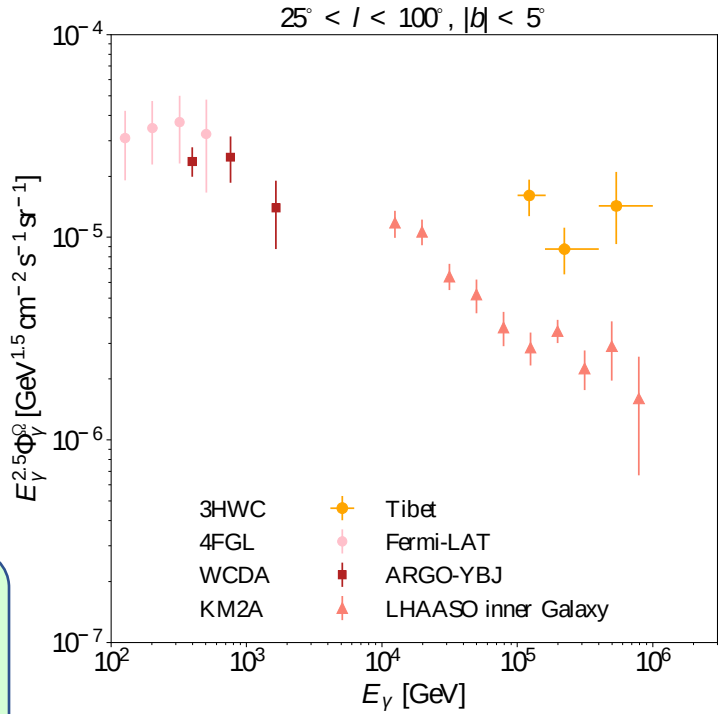

Interpretation of the Tibet & LHAASO GDE Fluxes

Kato et al., submitted to ApJL

$$\frac{\text{Tibet GDE } (25^\circ<l<100^\circ, |b|<5^\circ)-\text{Source}}{\text{LHAASO GDE}^{!} \ (15^\circ<l<125^\circ, |b|<5^\circ)} = 3, 2, \& \ 7 \ @ \ 120\text{TeV}, 220\text{TeV}, \& \ 530\text{TeV}$$

LHAAASO masking in the inner Galaxy[1]

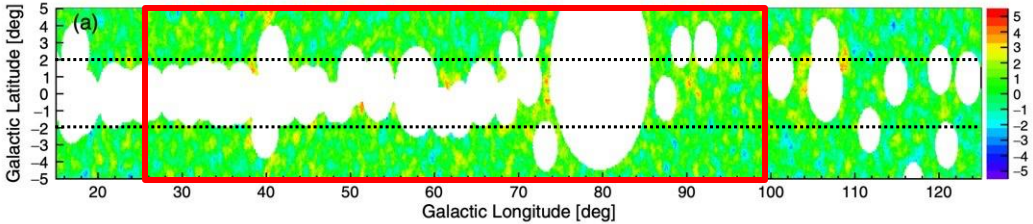

: Tibet region A ($25^\circ < l < 100^\circ$ & $|b| < 5^\circ$)

LHAASO masks most of the region w/i $|b| < 2^\circ$

1. Cao et al., PRL 131, 151001 (2023)
2. Lipari & Vernetto, PRD 98, 043003 (2018)

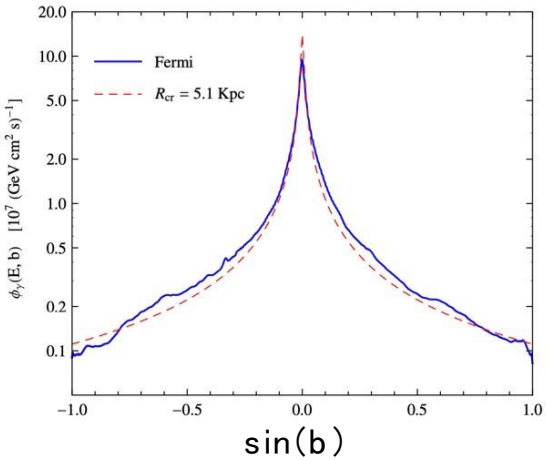

GDE latitudinal distribution*by Lipari & Vernetto (2018)[2]

*The distribution is Integrated over $|l| < 180^\circ$

Using the theoretical prediction,

$\underline{\text{Flux}(|b|<5^\circ)} \div \underline{\text{Flux}(2^\circ<|b|<5^\circ)} \sim 3$

~ Tibet region A ~ LHAASO inner Gal. plane

The following scenario can explain the difference:

They observe hadronic GDE, but in the different Galactic latitudinal regions due to their different masking schemes

1LHAASO Catalog and Tibet UHE Diffuse Events

Kato et al. ApJ, 961, L3 (2024)

• Tibet E > 400 TeV ◯ 1LHAASO UHE sources (95% containment radius)

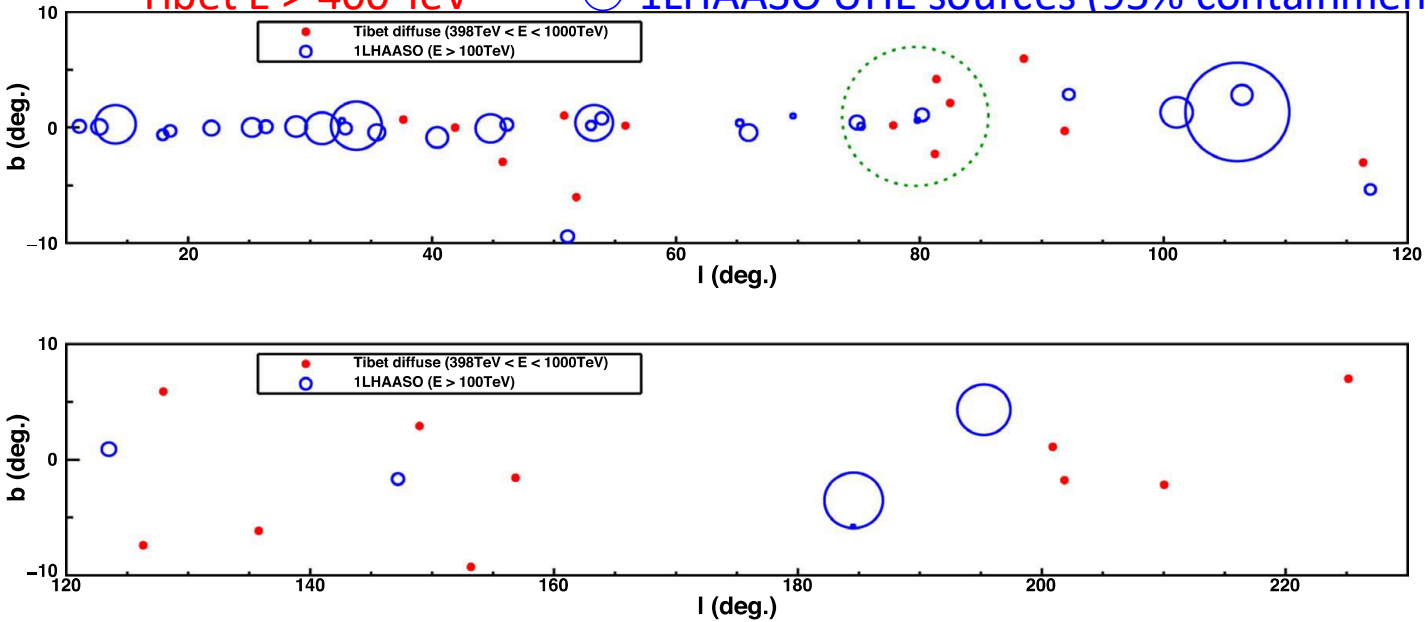

Tibet Galactic diffuse gamma rays above 400 TeV:
do NOT overlap with 1LHAASO UHE (>100 TeV) sources.
* Expected # of accidental overlap = 0.9 events

Source Contribution to the Tibet GDE Flux @ >100TeV

Kato et al., submitted to ApJL

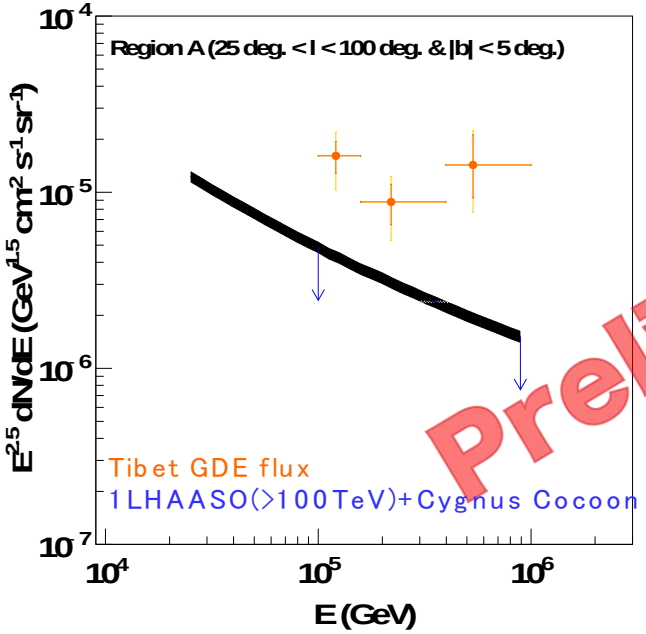

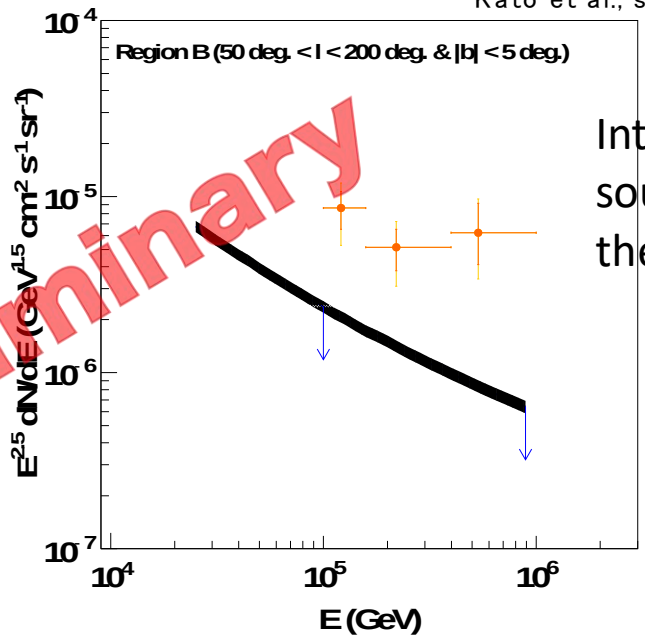

Integral fluxes of 1LHAASO sources (>100TeV) outside the Tibet masked region.

Source / Tibet GDE	Region A (25°<l<100° & |b|<5°)	Region B (50°<l<200° & |b|<5°)
121 TeV	< 26.9% ±9.9%	< 24.1% ±9.5%
220 TeV	< 34.8% ±14.0%	< 27.4% ±11.1%
534 TeV	$< 13.5\%^{+6.3\%}_{-7.7\%}$	$< 13.5\%^{+6.2\%}_{-7.6\%}$

Source contribution is subdominant

IceCube Diffuse Neutrinos

IceCube Collaboration: Science, 380, 1338 (2023)

4.5σ at Galactic plane

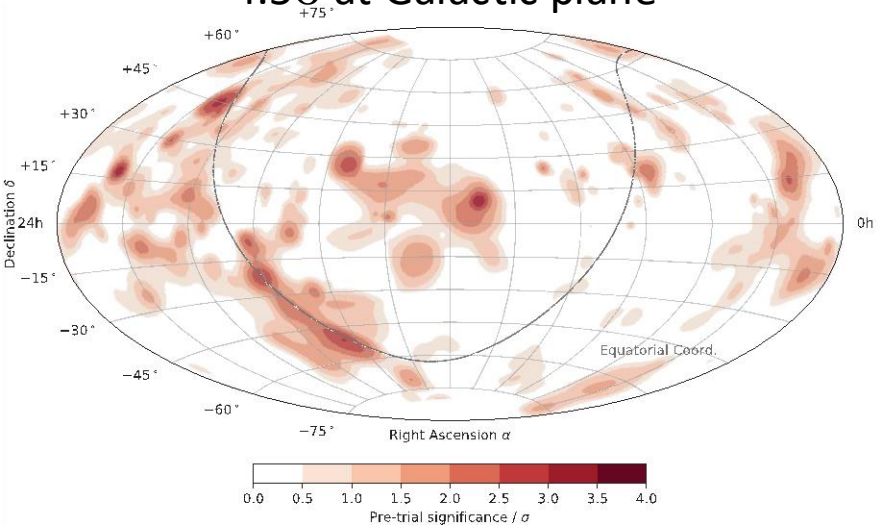

Comparison with Tibet diffuse γ-rays

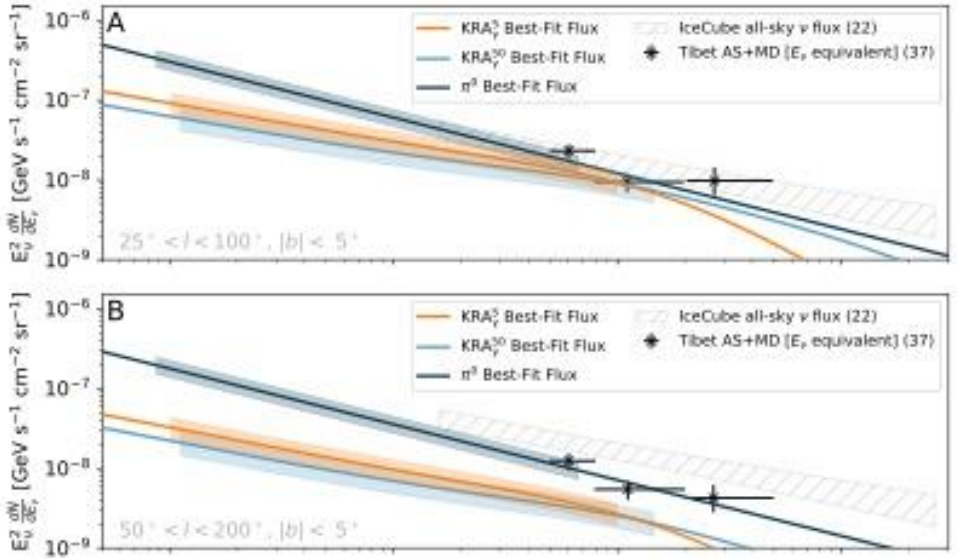

IceCube ν flux smoothly connects to the ν flux estimated from the Tibet sub-PeV γ-ray flux, assuming π^0-model best-fit flux supporting cosmic-ray origin of Tibet sub-PeV galactic diffuse γ rays.

PeVatron Candidate: SNR G106.3+2.7

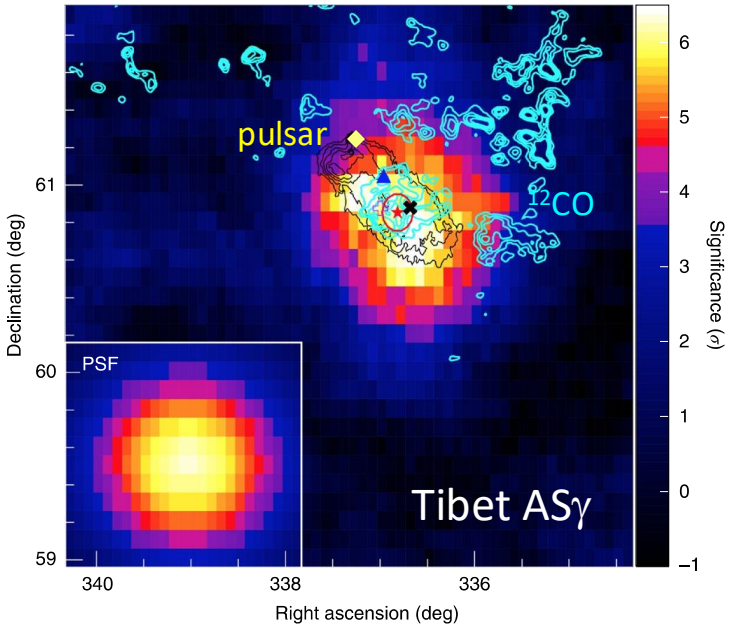

Detected by VERITAS, HAWC, Tibet ASγ, MAGIC, LHAASO

Amenomori et al., Nat. Astron (2021)

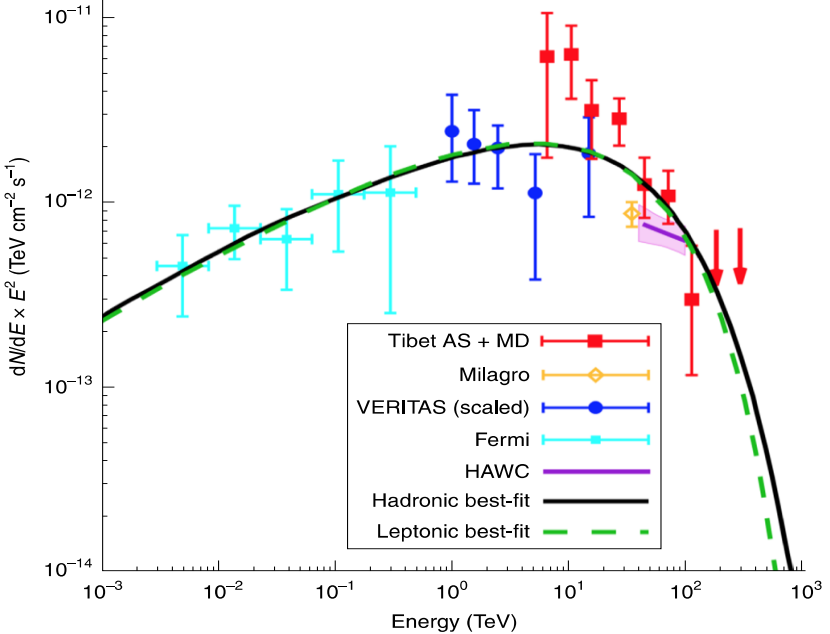

- ✓ Spectrum extends beyond 100 TeV (HAWC, Tibet ASγ, LHAASO) $E_{p,cut}$ = ~500 TeV
- ✓ Shell-type SNR near the pulsar (t_{age}~10kyr?, d=800pc?) W_p = ~5 x 10^{47} erg (>1GeV)
- ✓ Extended γ-ray excess ($\sigma_{EXT}=0.24^o \pm 0.10^o$)
- ✓ γ-ray excess is coincident with the molecular clouds (MCs) and SNR, not pulsar

MAGIC: SNR G106.3+2.7

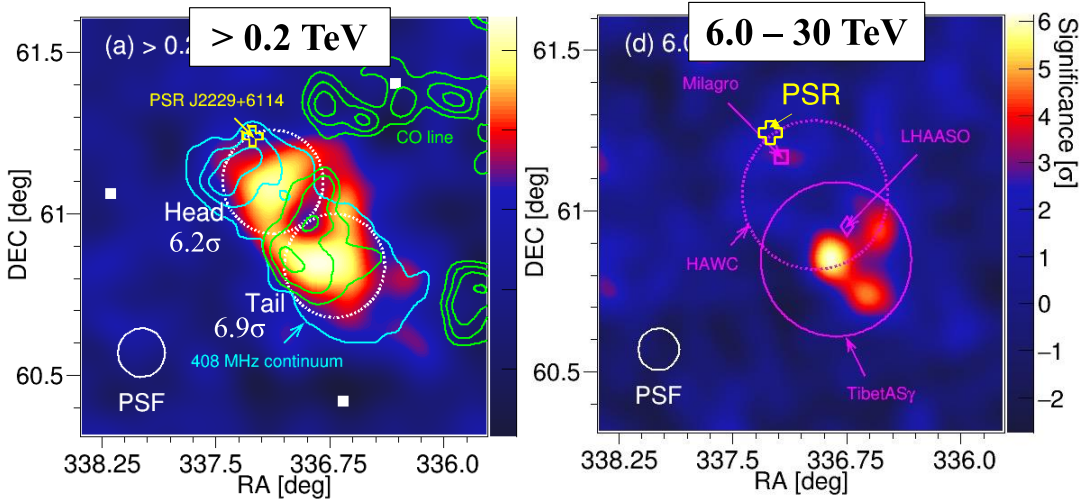

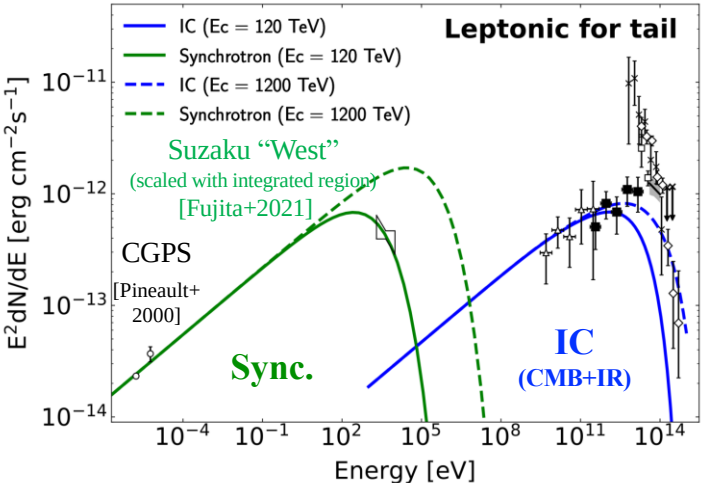

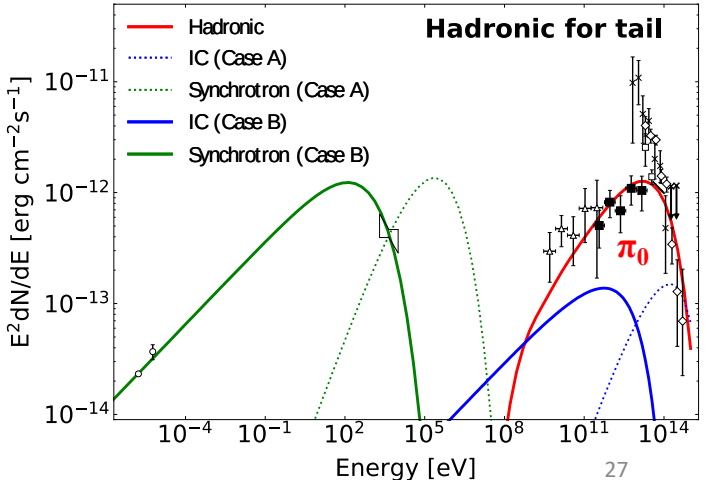

- ✓ HE emissions are consistent with Tibet ASγ
- ✓ SED for tail region favors hadronic model

Abe et al. (MAGIC Collab.), A&A, 671, 12 (2023)
Oka et al. (MAGIC Collab.), CTA workshop

PeVatron Candidate: HESS J1843-033

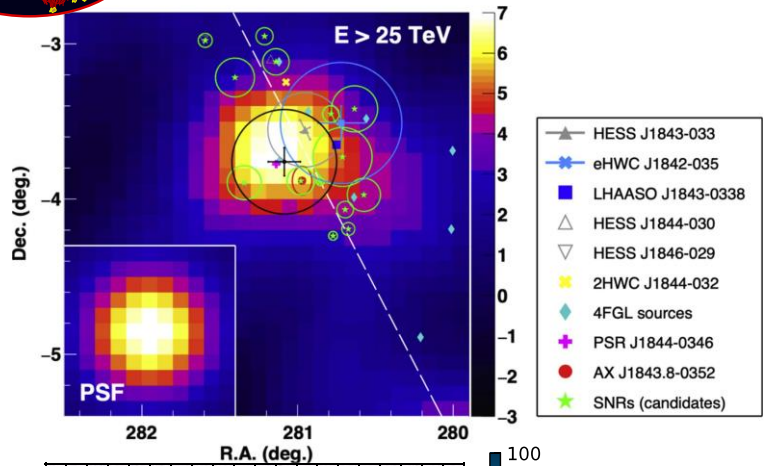

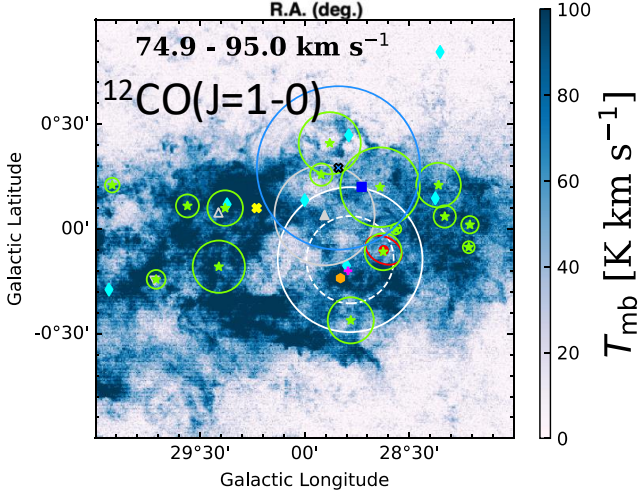

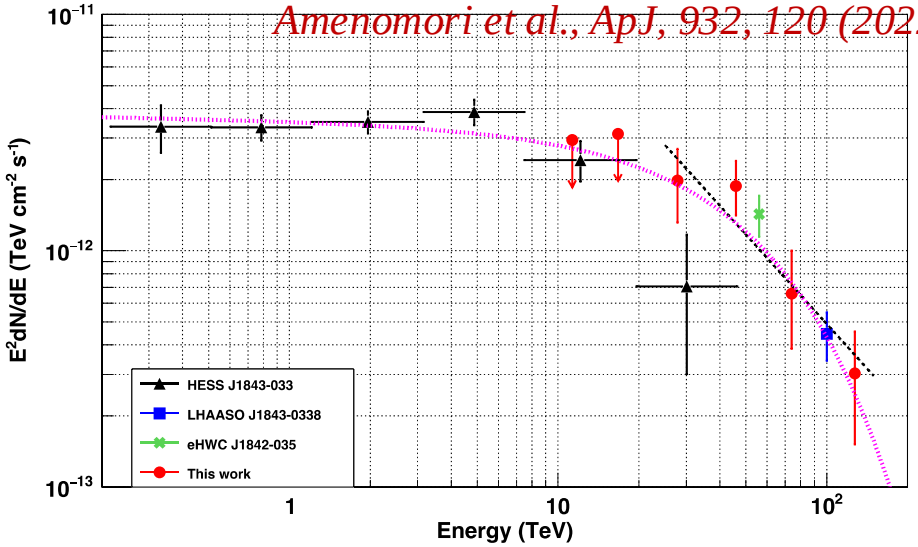

Candidate sources (Tage=2.7kyr?, d=9.6kpc)

- ✓ Shell-type SNR G28.6+0.1? or PSR J1844-00346?
- ✓ Extended γ-ray excess ($\sigma_{EXT}=0.34^o \pm 0.12^o$)
- ✓ γ-ray excess is coincident with the MCs
- ✓ Proton cutoff: ~500 TeV assuming the Hadronic model

W_p = ~6 x 10^{49} erg (>1TeV)

PeVatron Candidate: HESS J1849-000

Amenomori et al., ApJ, 954, 200 (2023)

- ✓ A middle-aged PWN (T_{age}=42.9kyr, d=7kpc)
- ✓ γ-ray excess is coincident with the MCs

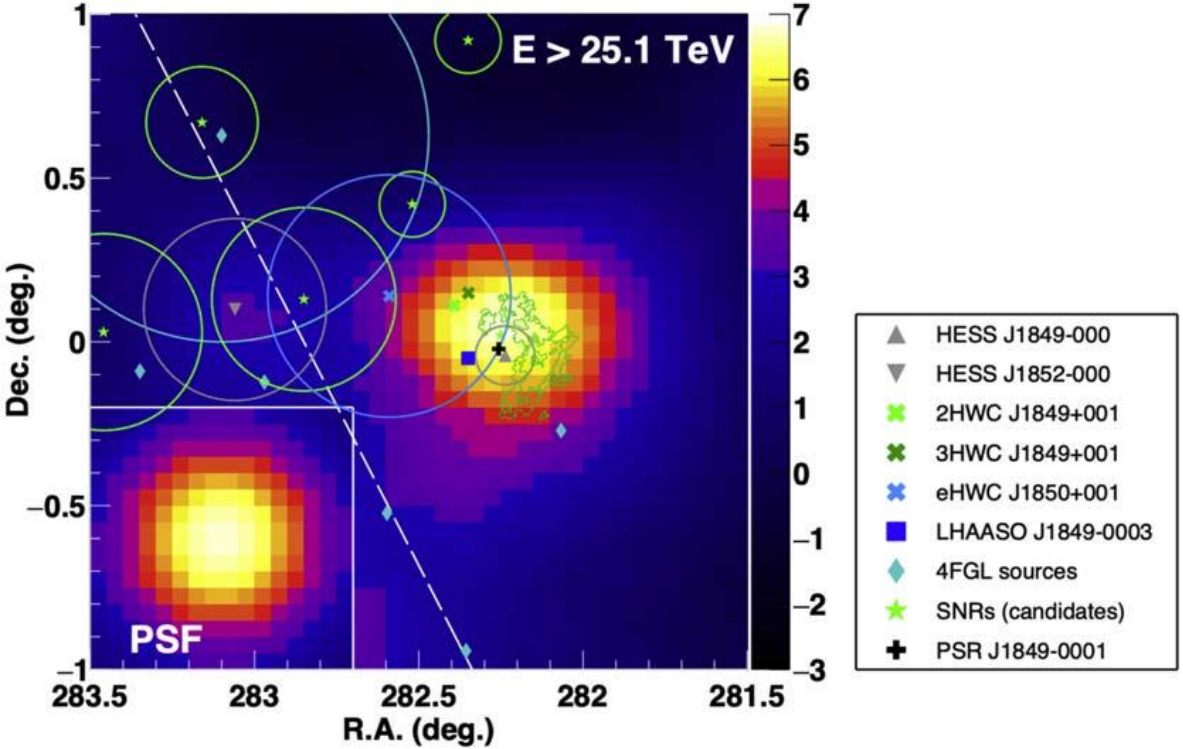

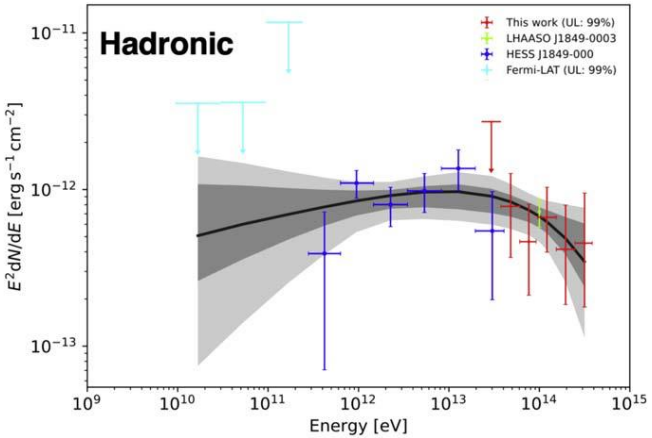

- ✓ Proton cutoff ~5 PeV assuming the Hadronic model W_p = ~1.1 x 10^{49} erg (>1TeV)
- ✓ Spectrum can be also modeled with the Leptonic scenario (IC)

Projects in the Southern Hemisphere

UHE diffuse gamma rays

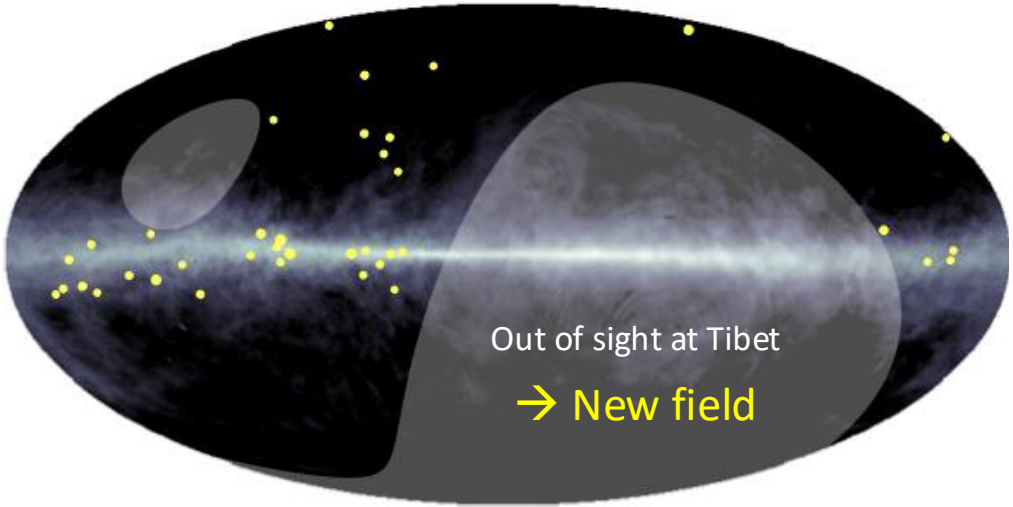

>40 UHE sources

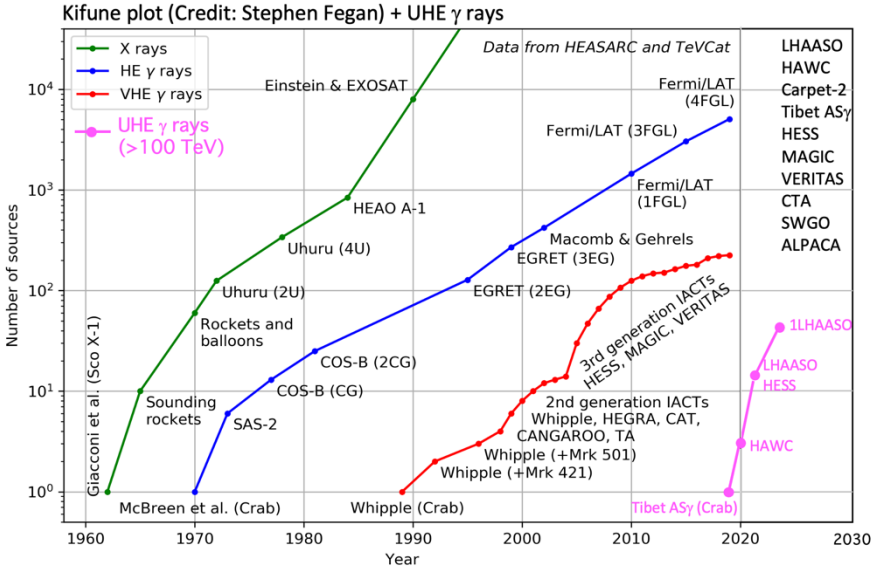

Draw the "Kifune" plot - the integral number of high energy sources detected as a function of year - in the style of a plot developed by Tadashi Kifune (for example http://adsabs.harvard.edu/abs/1996NCimC..19..953K).
The data for the number of X-ray and HE (GeV) gamma-ray sources come from a page on HEASARC maintained by Stephen A. Drake (retrieved 2017-09-28) : https://heasarc.gsfc.nasa.gov/docs/heasarc/headates/how_many_xray.html
The data for the number of VHE (TeV) gamma-ray sources is from TeVCat maintained by Deirdre Horan and Scott Wakely (retrieved 2017-09-28) : http://tevcat.uchicago.edu/

Go South!

(e.g., ALPACA [2024-25], Mega ALPACA, SWGO, CTA, …) & Neutrinos

Conclusions

- ✓ Tibet ASγ experiment successfully observed UHE gamma rays from the Crab Nebula for the first time and opened new energy window. (Now >40 UHE γ ray sources detected by LHAASO, HAWC, H.E.S.S. and Tibet ASγ)
- ✓ Tibet ASγ experiment successfully observed Galactic diffuse gamma rays between 100 TeV and 1 PeV for the first time.
- ✓ Tibet UHE events (>400 TeV) do not originate from LHAASO UHE (>100 TeV) sources. Possible source contribution from LHAASO UHE sources is less than 20-30%.
- ✓ IceCube diffuse neutrino flux smoothly connects to Tibet ASγ diffuse gamma-ray flux assuming π^0 best-fit model supporting the cosmic-ray origin.
- ✓ Tibet ASγ experiment measured the energy spectra of a few PeVatron candidates associated with the molecular clouds.

These facts indicate strong evidence that cosmic rays are accelerated beyond PeV energies in our Galaxy and spread over the Galactic disk.
→ Search for more PeVatron candidates! → Go South!

Backup slides

Projects in the Southern Hemisphere

ALPACA experiment

Bolivia

Chacaltaya plateau

4740m a.s.l

(16° 23’ S, 68° 08’ W)

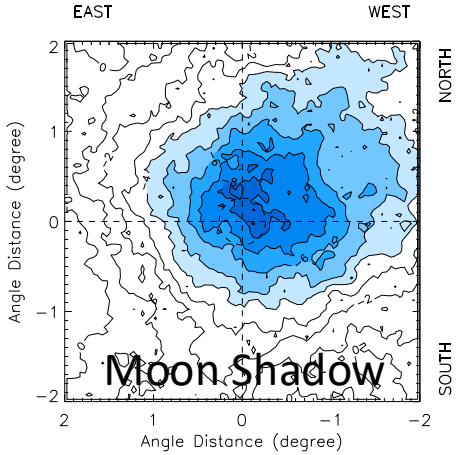

Kawata, et al, ICRC2023

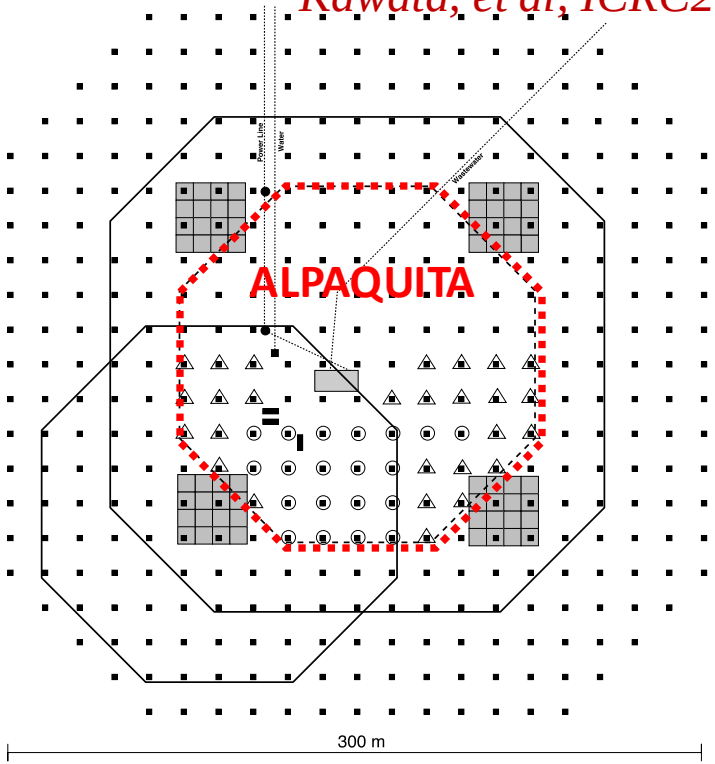

Go South!

(e.g., ALPACA [2024-25], Mega ALPACA, SWGO, CTA, …) & Neutrinos

Composition Dependence

CRs interact with interstellar gas
(γ-ray energy has 10% of CRs)

$$CR + ISM \rightarrow X\text{'s} + \pi^0 \ldots \rightarrow 2\gamma$$

→ Diffuse gamma-ray spectrum depends on the CR composition

Vernetto & Lipari (ICRC2021)

factor 1.5 – 2 difference@~600 TeV

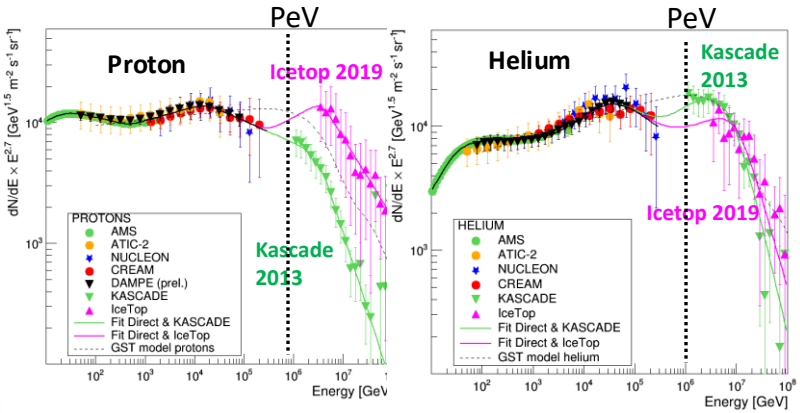

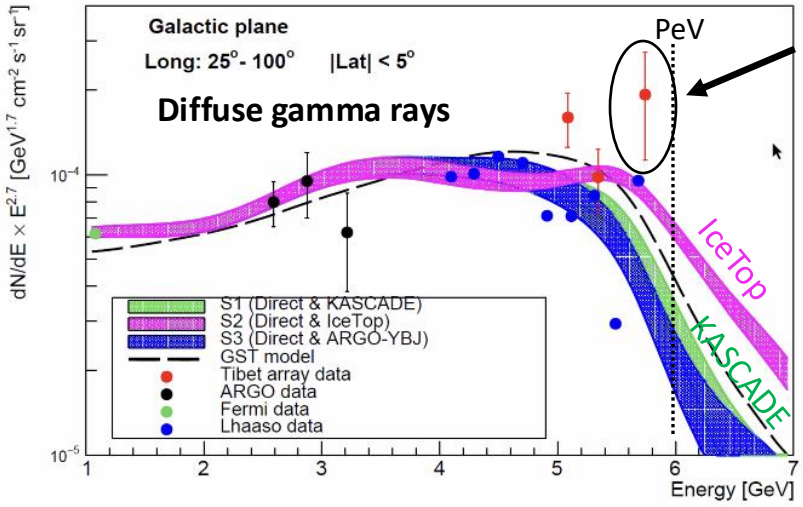

4 ev / 10 ev from Cygnus cocoon (< 4°)

Data Table

TABLE S1. Number of events observed by the Tibet AS+MD array in the direction of the galactic plane. The galactic longitude of the arrival direction is integrated across our field of view (approximately $22^\circ < l < 225^\circ$). The ratios (α) of exposures between the ON and OFF regions are 0.135 for $|b| < 5^\circ$ and 0.27 for $|b| < 10^\circ$, respectively.

	$\|b\| < 5^\circ$			$\|b\| < 10^\circ$		
Energy bin (TeV)	$N_{\rm ON}$	$N_{\rm BG}$ $(= \alpha N_{\rm OFF})$	Significance (σ)	$N_{\rm ON}$	$N_{\rm BG}$ $(= \alpha N_{\rm OFF})$	Significance (σ)
$100 - 158$	513	333	8.5	858	655	6.6
$158 - 398$	117	58.1	6.3	182	114	5.1
$398 - 1000$	16	1.35	6.0	23	2.73	5.9

TABLE S2. Galactic diffuse gamma-ray fluxes measured by the Tibet AS+MD array.

Energy bin (TeV)	Representative E (TeV)	Flux $(25^\circ < l < 100^\circ, \|b\| < 5^\circ)$ $(\mathrm{TeV}^{-1}\ \mathrm{cm}^{-2}\ \mathrm{s}^{-1}\ \mathrm{sr}^{-1})$	Flux $(50^\circ < l < 200^\circ, \|b\| < 5^\circ)$ $(\mathrm{TeV}^{-1}\ \mathrm{cm}^{-2}\ \mathrm{s}^{-1}\ \mathrm{sr}^{-1})$
$100 - 158$	121	$(3.16 \pm 0.64) \times 10^{-15}$	$(1.69 \pm 0.41) \times 10^{-15}$
$158 - 398$	220	$(3.88 \pm 1.00) \times 10^{-16}$	$(2.27 \pm 0.60) \times 10^{-16}$
$398 - 1000$	534	$(6.86\ ^{+3.30}_{-2.40}) \times 10^{-17}$	$(2.99\ ^{+1.40}_{-1.02}) \times 10^{-17}$

Angular/Energy Resolutions

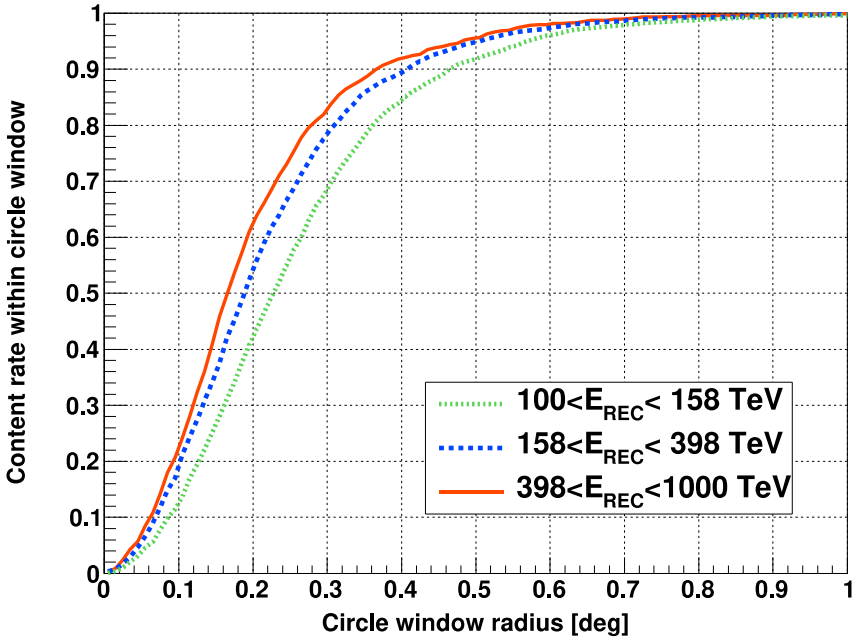

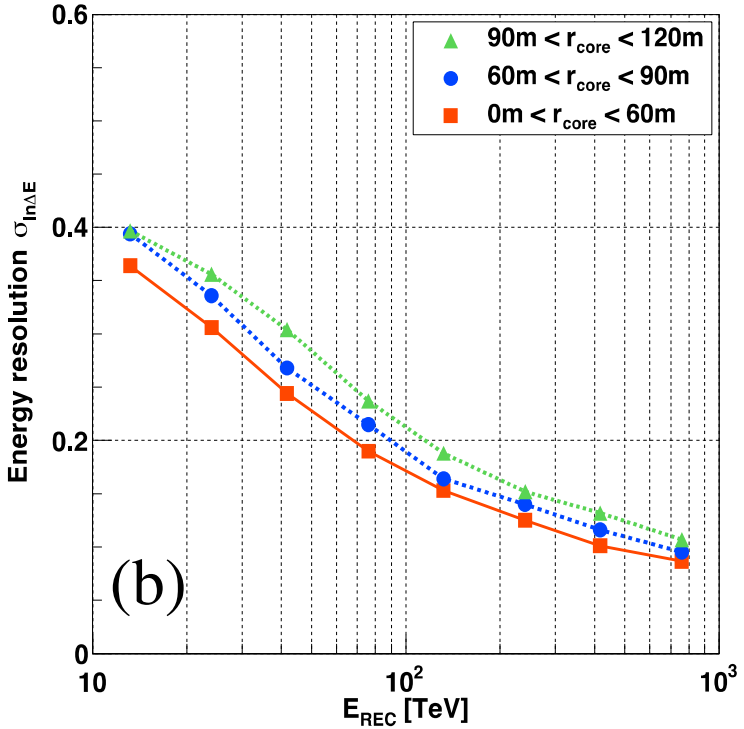

CASA-MIA Observation

TABLE 1

LIMITS TO DIFFUSE EMISSION

Region ($50° < l < 200°$)	Median Energy (TeV)	Significance (σ)	J_γ/J_{CR} 90% C.L. (10^{-5})
$-2° < b < 2°$	140	+1.78	7.2
	180	+1.81	3.8
	310	+2.56	5.2
	650	+1.12	3.2
	1300	+0.07	4.6
$-5° < b < 5°$	140	+1.63	3.4
	180	+0.08	2.6
	310	+0.86	2.4
	650	+1.60	2.6
	1300	+0.06	3.5
$-10° < b < 10°$	140	+2.39	2.8
	180	+1.79	2.2
	310	+0.87	2.3
	650	+0.91	1.8
	1300	−0.56	2.3

NOTE.—Tabulated upper limits to diffuse gamma-ray emission from the plane of the Galaxy. Although positive excesses are seen, we do not view these as statistically significant enough to claim detections. Flux limits are tabulated for bands along the Galactic plane from $|b| < 2°$ to $|b| < 10°$. Median energy is quoted for integral flux limits. Selected spatial regions and energy bands are not statistically independent.

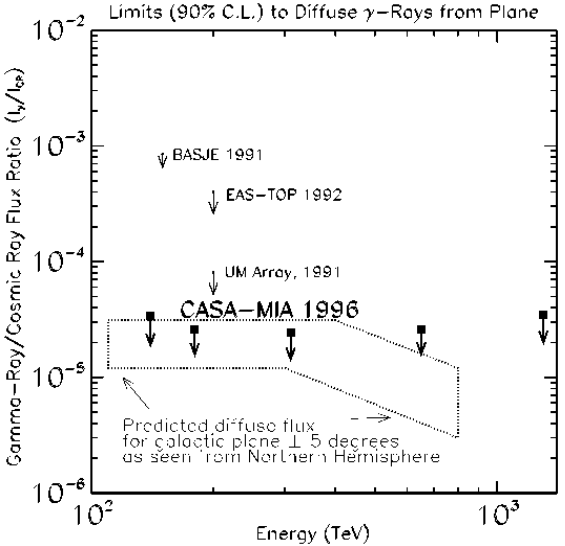

FIG. 4.—CASA-MIA sensitivity to diffuse gamma-ray emission from the central plane of the Galaxy ($|b| < \pm 5°$, $50° < l < 200°$). Sensitivities are given in terms of the fraction of gamma rays relative to the detected all-particle flux of cosmic rays at the Earth. Also shown are limits from previous experiments (BASJE—Kakimoto et al. 1991; EAS-TOP—Aglietta et al. 1992, UM—Matthews et al. 1991). Predicted flux from Aharonian (1991).

Borione et al., Astrophys. J. 493, 175 (1998)

$[I_\gamma] / [I_{CR}] \sim 3 \times 10^{-5}$

Diffuse Model

Lipari & Vernetto, PRD (2018)

Model can reproduce global structure
(not considered of the local structures)

Gas density

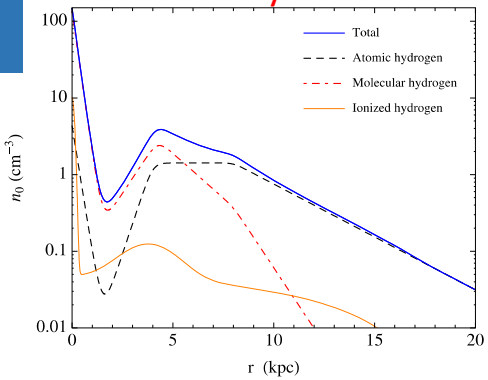

Cosmic rays

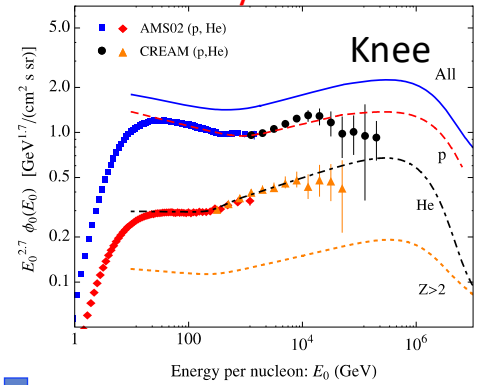

Electrons+Positrons

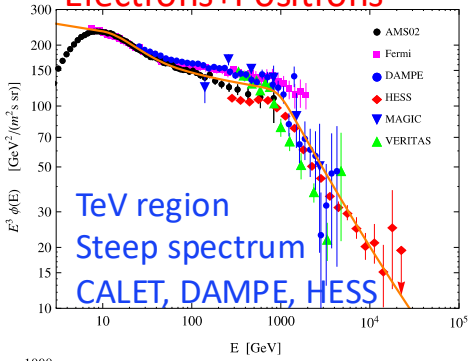

TeV region
Steep spectrum
CALET, DAMPE, HESS

Photon density

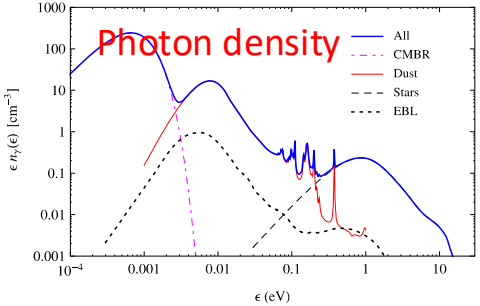

Brems.

Compton

Hadronic

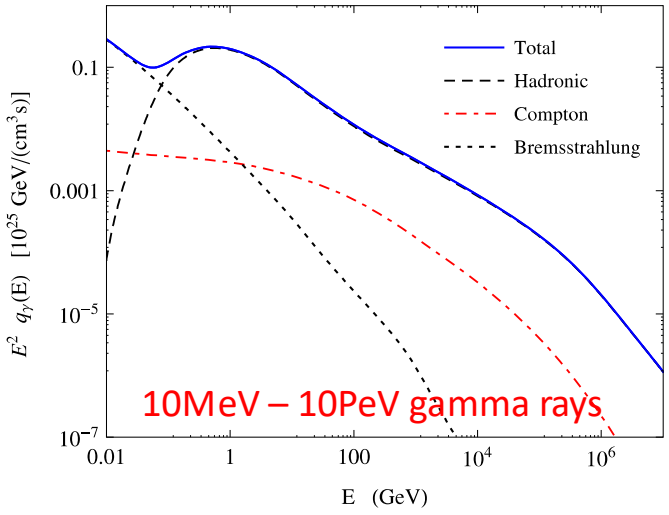

10MeV – 10PeV gamma rays

Cosmic Ray Pool × ISM

High-energy cosmic rays

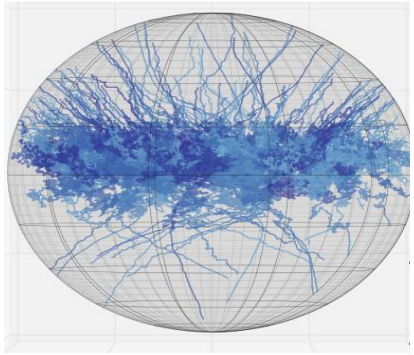

Figure from slide presented by A. Kääpä (Bergische Universität Wuppertal) at CRA2019 workshop

×

Interstellar matter

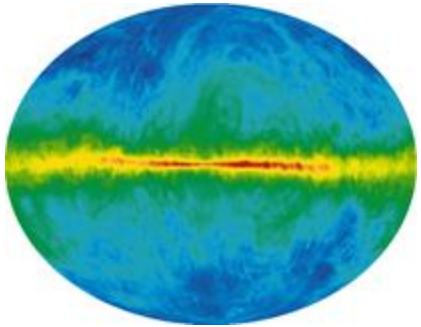

Radio (21cm) HI Map
Hartmann et al. (1997)
Dickey & Lockman (1990)

=

High-energy gamma rays

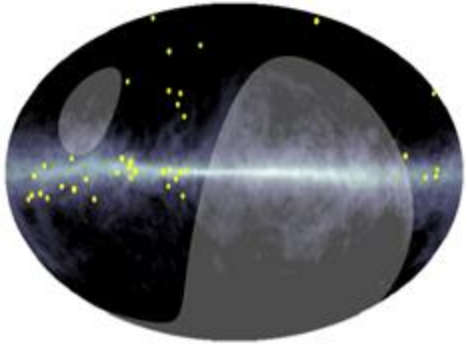

This Work

✓ This work proves a theoretical model that cosmic rays produced by PeVatrons are trapped in the Galactic magnetic field for millions of years, forming a pool of cosmic rays.

Reproducing Fermi-LAT Results

Model can reproduce global structure
(not taken into account of local structure)

Lipari & Vernetto, PRD (2018)

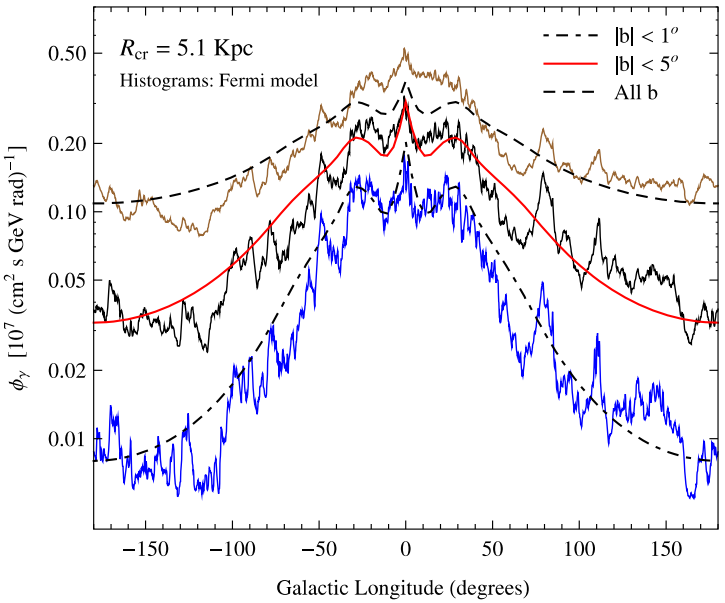

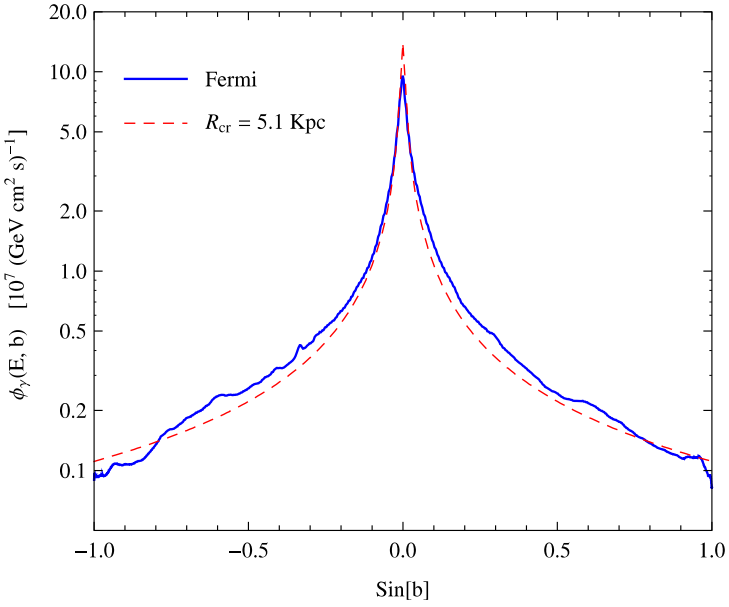

Space Dependence of CR Spectrum

Lipari & Vernetto, PRD (2018)

Harder gamma-ray spectral index, getting closer to the G.C. @12 GeV

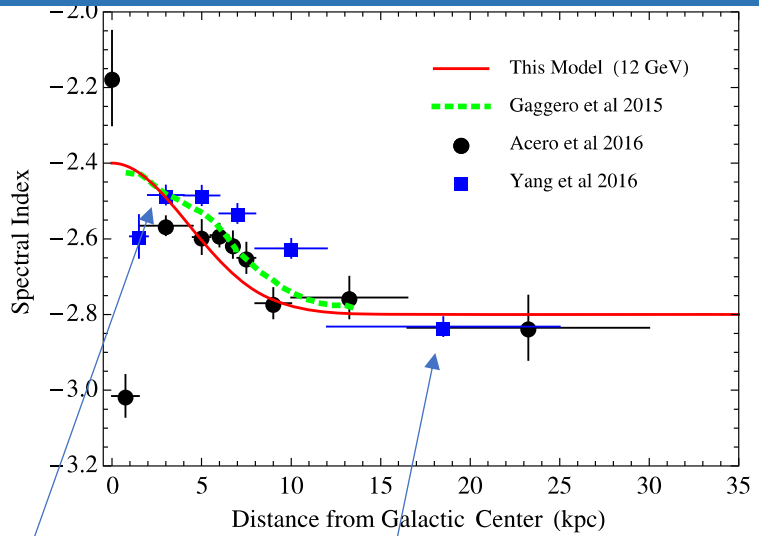

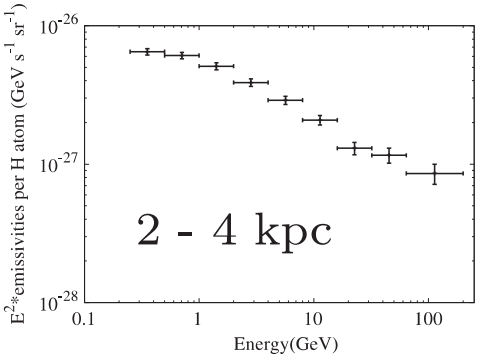

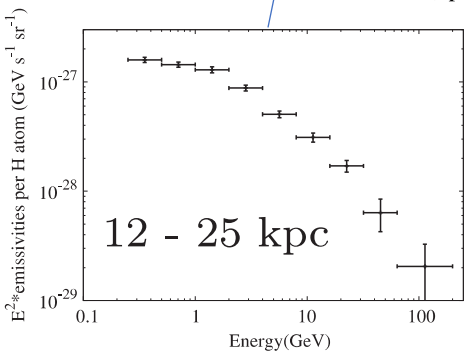

Yang et al., Phys. Rev. D 93, 123007 (2016)

Muon Number Distribution (>398 TeV)

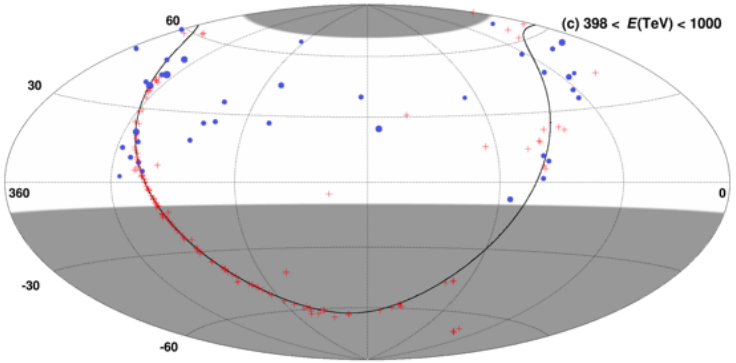

• ON region $|b| < 10^{o}$

BG region $|b| > 20^{o}$

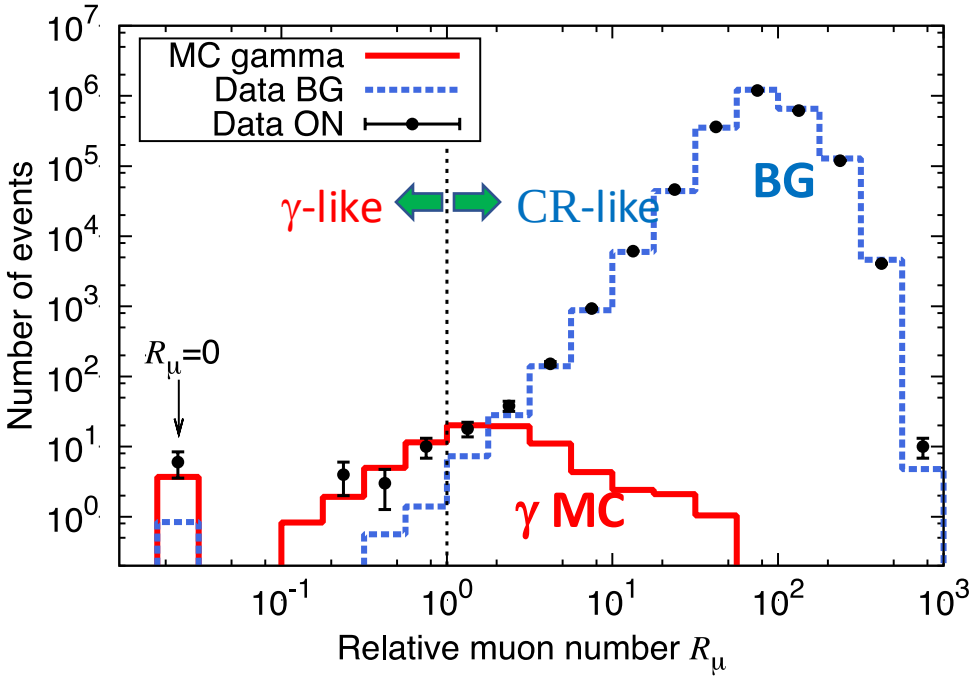

Gamma Survival ratio :

30% by MC sim (>398TeV)

CR Survival ratio :

~10^{-6} (>398TeV=$10^{2.6}$TeV)

$$R\mu = \frac{\text{Observed \# of muons}}{\text{\# of muons at the cut value}}$$

How to Identify PeVatrons

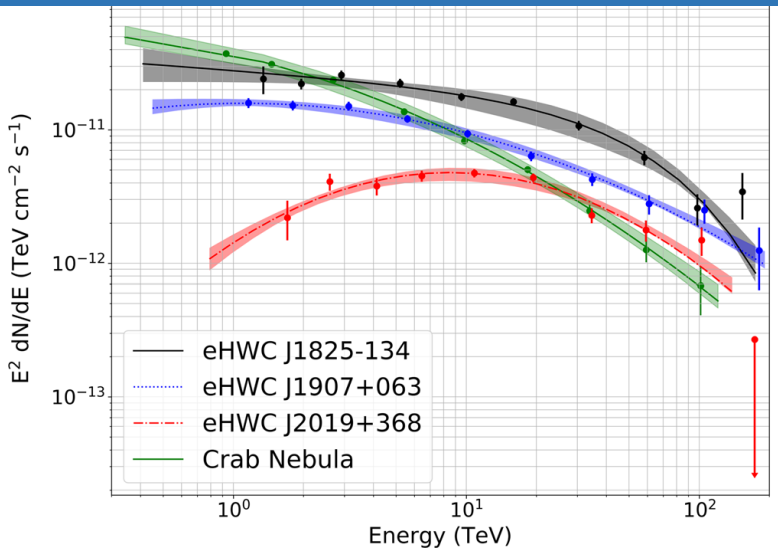

eHWC J1825-134 (PWN?)
PSR J1826-1334
PSR J1826-1256
A few SNRs …

eHWC J1907+063 (PWN?)
PSR J1907+0602
SNR G40.5-0.5

eHWC J2019+368 (PWN?)

✓ Hard spectral index (~ -2)
✓ Extended morphology

Source name	RA (°)	Dec (°)	Extension > 56 TeV (°)	F (10^{-14} ph cm^{-2} s^{-1})	$\sqrt{TS}$ > 56 TeV	Nearest 2HWC source	Distance to 2HWC source(°)	$\sqrt{TS}$ > 100 TeV
eHWC J0534 + 220	83.61 ± 0.02	22.00 ± 0.03	PS	1.2 ± 0.2	12.0	J0534 + 220	0.02	4.44
eHWC J1809 − 193	272.46 ± 0.13	−19.34 ± 0.14	0.34 ± 0.13	$2.4^{+0.6}_{-0.5}$	6.97	J1809 − 190	0.30	4.82
eHWC J1825 − 134	276.40 ± 0.06	−13.37 ± 0.06	0.36 ± 0.05	4.6 ± 0.5	14.5	J1825 − 134	0.07	7.33
eHWC J1839 − 057	279.77 ± 0.12	−5.71 ± 0.10	0.34 ± 0.08	1.5 ± 0.3	7.03	J1837 − 065	0.96	3.06
eHWC J1842 − 035	280.72 ± 0.15	−3.51 ± 0.11	0.39 ± 0.09	1.5 ± 0.3	6.63	J1844 − 032	0.44	2.70
eHWC J1850 + 001	282.59 ± 0.21	0.14 ± 0.12	0.37 ± 0.16	$1.1^{+0.3}_{-0.2}$	5.31	J1849 + 001	0.20	3.04
eHWC J1907 + 063	286.91 ± 0.10	6.32 ± 0.09	0.52 ± 0.09	2.8 ± 0.4	10.4	J1908 + 063	0.16	7.30
eHWC J2019 + 368	304.95 ± 0.07	36.78 ± 0.04	0.20 ± 0.05	$1.6^{+0.3}_{-0.2}$	10.2	J2019 + 367	0.02	4.85
eHWC J2030 + 412	307.74 ± 0.09	41.23 ± 0.07	0.18 ± 0.06	0.9 ± 0.2	6.43	J2031 + 415	0.34	3.07

Abeysekara et al., PRL, 124, 021102 (2020)

PeVatron Candidate: SNR G106.3+2.7

Amenomori et al., Nat. Astron (2021)

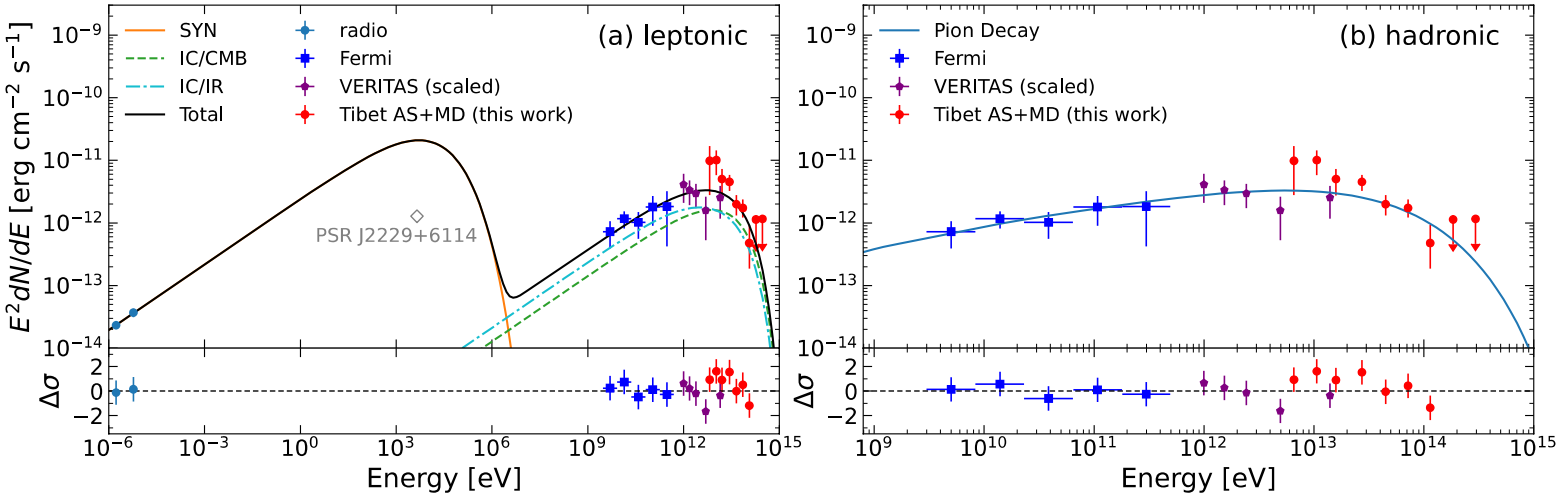

Electron spectrum: α=-2.3, E_{cut}=190TeV
Magnetic field: B=8.6μG
→ Cooling time τ_{sync}=0.9kyr << SNR age 10kyr

The required total energy of electrons is $\sim 1.4 \times 10^{47}$ erg, which only takes up ~ 2% of the spin-down energy released in the entire pulsar lifetime. If the rest of the spin-down energy goes into the magnetic field, the average magnetic field in the PWN would be much larger than the required value of 8 μG and results in very large fluxes at radio and X-ray wavelengths.

Pulsar Halo Model of Diffuse γ-Rays

Tim Linden and Benjamin J. Buckman, PHYSICAL REVIEW LETTERS 120, 121101 (2018)

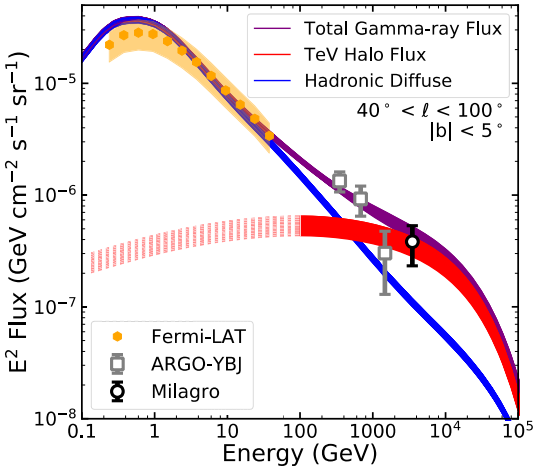

FIG. 1. The contribution of subthreshold TeV halos to the diffuse γ-ray emission along the galactic plane in the region $40° < \ell < 100°$, and $|b| < 5°$, compared to observations by the Fermi-LAT (described in the text), ARGO-YBJ [5], and Milagro [1]. The background (blue) corresponds to the predictions of 128 GALPROP models of diffuse γ-ray emission [8]. The contribution from TeV halos (red) is described in the text. TeV halos naturally reproduce the TeV excess observed by Milagro, while remaining consistent with ARGO-YBJ observations. The dashed red region indicates our ignorance of low-energy γ-ray emission from TeV halos.

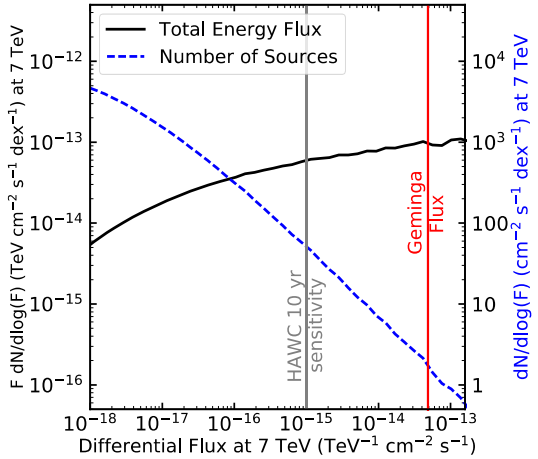

FIG. 3. The contribution of individual TeV halos to the TeV excess in the region $40° < \ell < 100°$, and $|b| < 5°$. We normalize our results at 7 TeV [19], assuming that individual TeV halos convert their spin-down luminosity into 7 TeV γ rays with an identical efficiency as Geminga. Vertical lines correspond to the flux of Geminga, and the projected 10 yr HAWC sensitivity. Results are shown for the total γ-ray flux $[FdN/d\log_{10}(F)$, black, left y axis], which indicates that most of the γ-ray intensity stems from the bright TeV halos, as well as for the source count $[dN/d\log_{10}(F)$, blue, right y axis], which indicates that 10 yr HAWC data will observe ~50 TeV halos in the ROI. For illustrative purposes, in this plot we show the contribution from TeV halos with individual fluxes exceeding Geminga, predicting the existence of only ~1 such system.

Data/MC Comparison

- ✓ AS generation: CORSIKA
- ✓ Hadronic int. model: EPOS-LHC + FLUKA
- ✓ Detectors: GEANT4

Reasonable agreement!

*Note: Cosmic-ray MC simulation is not used for the flux calculation or for any optimization of the analysis.

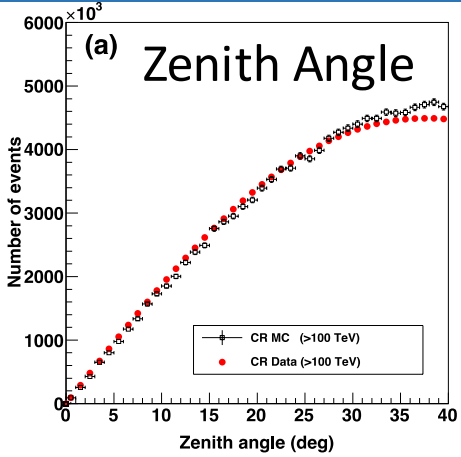

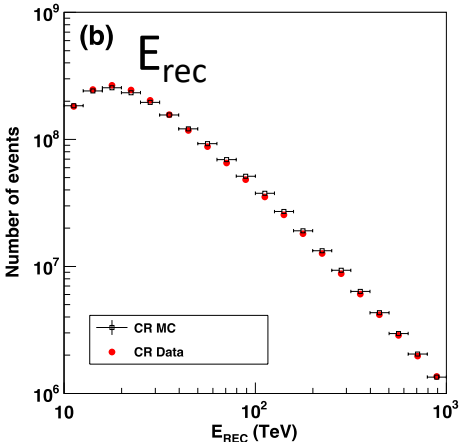

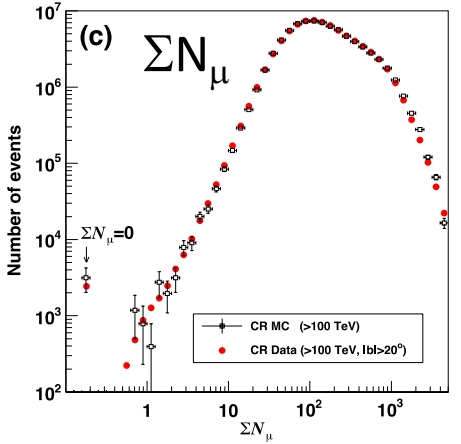

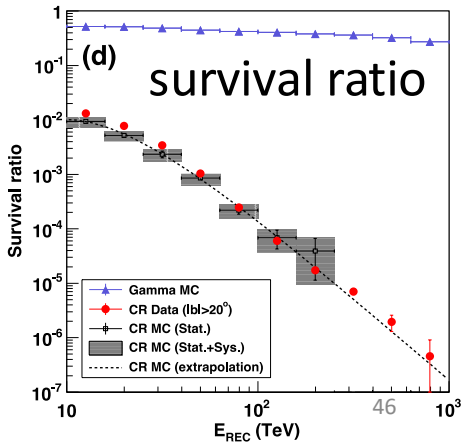

How to Identify PeVatrons

Spectrum example
TeV J2032+4130

X-ray Satellites
γ-ray Satellites
IACTs
EAS Arrays

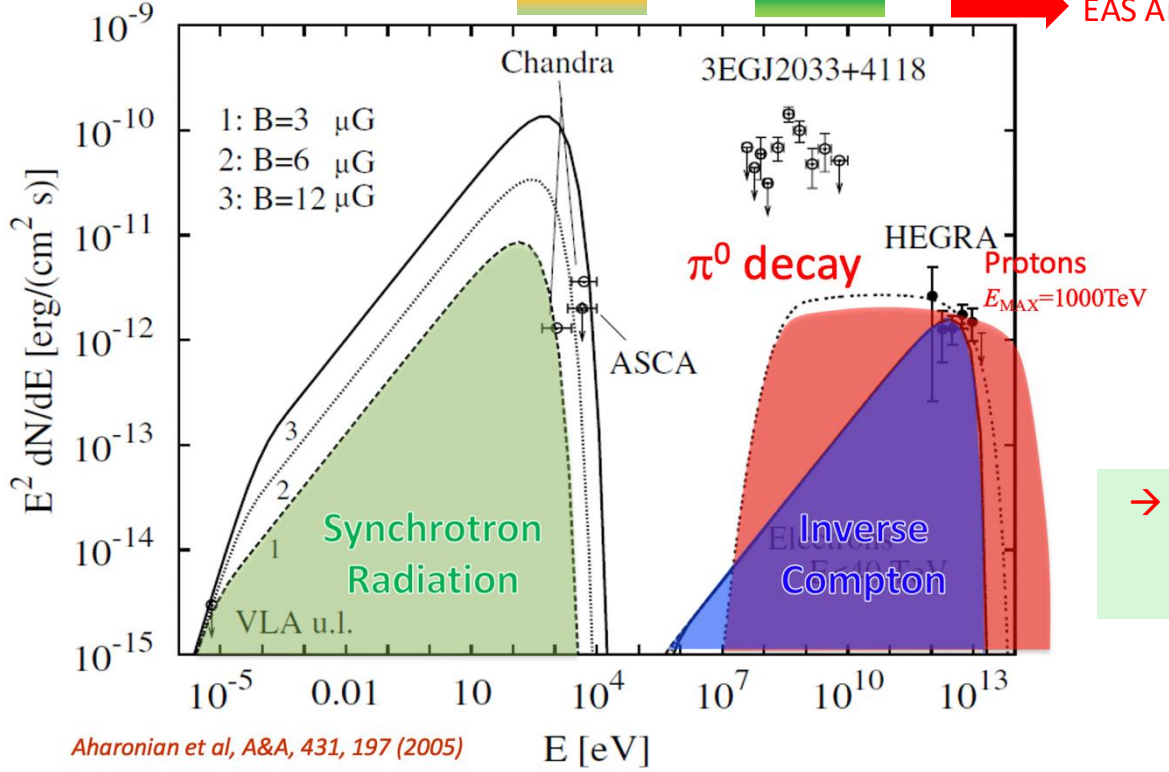

→ Hard spectral index (−2) beyond 100 TeV (+ Molecular Cloud)

How to Identify PeVatrons

- γ-ray beyond 100 TeV by Tibet, HAWC etc. in North,
  ALPACA, SWGO in south will come soon
- Spectral index $\alpha \sim -2$ in TeV by IACTs
- Coincident with molecular cloud observed by radio
- π^0 cutoff around 70 MeV by γ-ray satellites
- Dark in X-ray observation
- Deep observation by IACTs to resolve sources
- Coincident with HE neutrino by IceCube

Multi-wavelength Multi-particle Observations

Cygnus OB1 & OB2 in the 100 TeV region

Amenomori et al., PRL, 127, 031102 (2021)

Cyg. OB2

Cyg. OB1

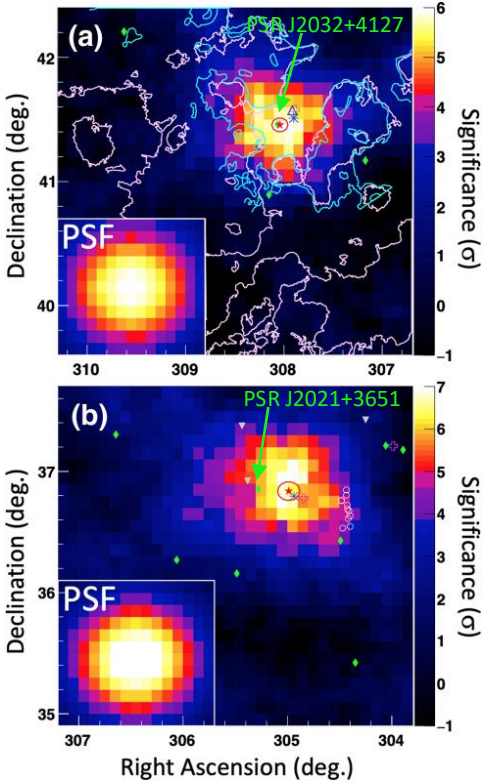

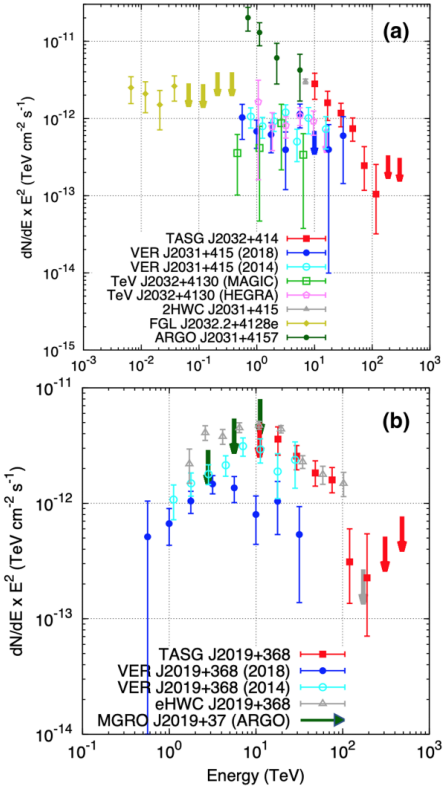

Molecular Cloud around HESS J1849-000

Detection of a Molecular Cloud

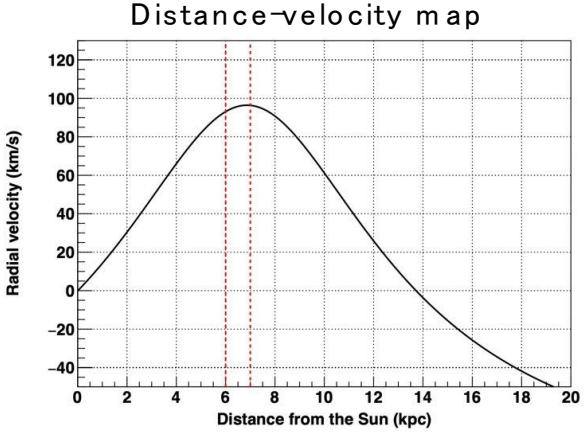

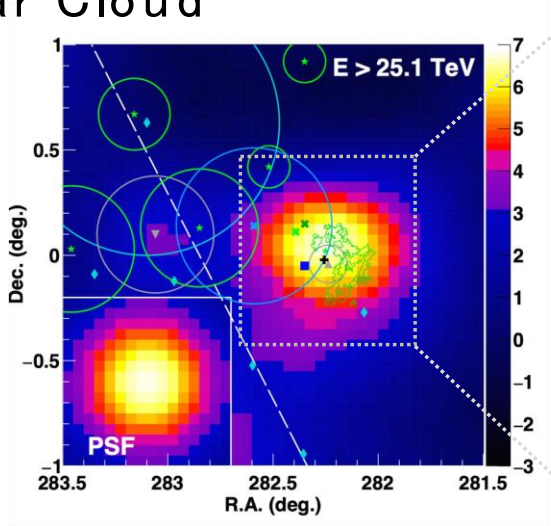

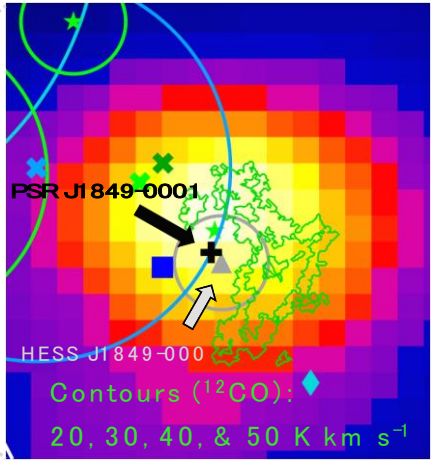

- Analysis of archive ^{12}CO (J=1-0) data (FUGIN[1])
- Assumed istance: 7 kpc[2]
- Integration of velocity range of 93-100 km s^{-1}

  => A ~20 pc size cloud w/ T_b ~20 K km s^{-1} @ the west of HESS J1849-000
- Overlap b/w γ-ray emission & cloud
- Gas density: np = Xco T_{mb} / R ~ 70 cm^{-3} (Xco = 2 ×10^{20} cm^{-2} (K km s^{-1})$^{-1}$)[3]

  => Can provide the gas density of ≳ 10 cm^{-3}

1. Umemoto+, PASJ 69, 5 (2017)
2. Gotthelf+, ApJL 729, L16 (2011)
3. Bolatto+, Ann. Rev. Astron. Astrophys 51, 207 (2013)

Adiabatic Compression for HESS J1849-000

Possible Acceleration Mechanism of PeV CRs

✓ CR acceleration in a **PWN-SNR composite system**[1,2] ??

- CR protons pre-accelerated up to ~100 TeV in the SNR FS are re-accelerated up to ~ 1 PeV in the PWN compressed by the SNR reverse shock
- ~10^{49} erg is given to the accelerated particles[1]
- PWN is compressed to ~10% of the original size[1,2]
- B of the PWN is amplified up to ~ 100 μG[1]
  => compact synchrotron X-ray emission by $e^{\pm}$ of PWN origin??

Evolution of the size of the system

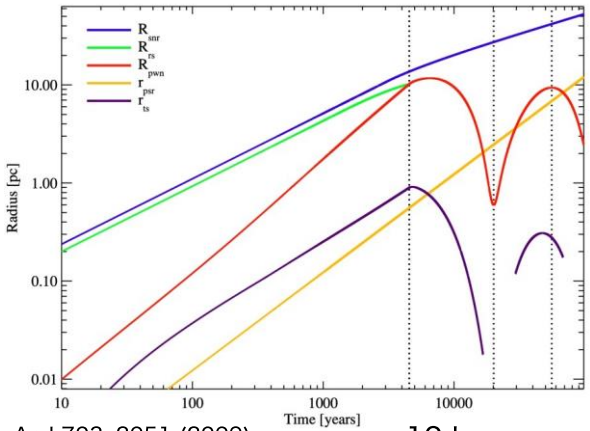

10 kyr

Energy spectrum of CR protons[2]
(Initially injected w/ 100 TeV mono energy)

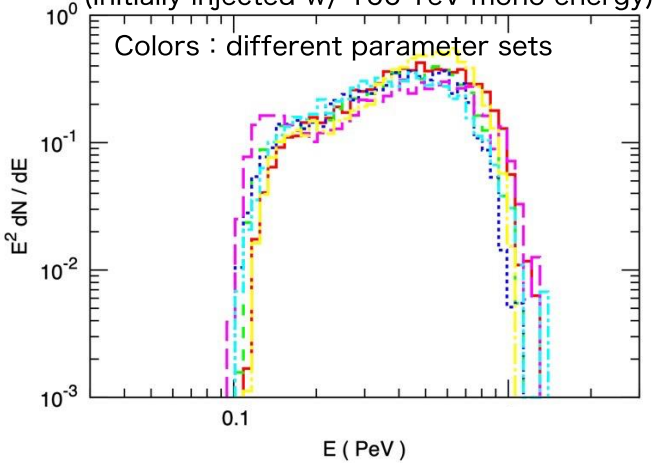

1. Gelfand+, ApJ 703, 2051 (2009)
2. Ohira+, MNRAS 478, 926 (2018)

TASG J1844-038

Discussion (1): Association of TASG J1844-038 w/ SNR G28.6-0.1 (1)

SNR G28.6-0.1

- Nonthermal radio[1] & X-rays[2] by electron synchrotron radiation
- Shell-type SNR[2]
- Distance: 9.6±0.3 kpc[3]
- Age: 2.7 kyr[2] or 19 kyr[3]

TASG J1844-038's radius: $\sigma = 0.34° \pm 0.12°$

AX J1843.8-0352's radius (X-rays): $\sigma_{mean} = 0.075^{o}$ (4.5')[4]

Discrepancy in their extensions at the 2.3 σ level

=> Contribution of gamma rays of hadronic origin ? (CR interaction w/ ambient molecular clouds ?)

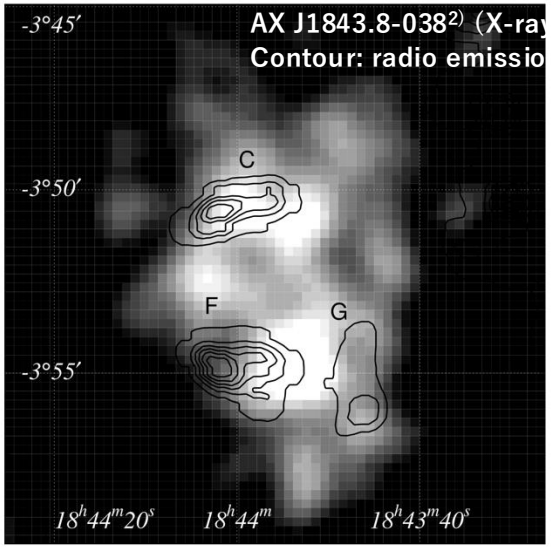

1) Helfand et al., ApJ 341, 151 (1989)
2) Bamba et al., PASJ 53, L21 (2001)
3) Ranasinghe & Leahy, MNRAS 477, 2243 (2018)
4) Ueno et al., ApJ 588, 338 (2003)

TASG J1844-038

Discussion (1): Association of TASG J1844-038 w/ SNR G28.6-0.1 (2)

^{12}CO (J = 1 - 0) map from the FUGIN data[1)]

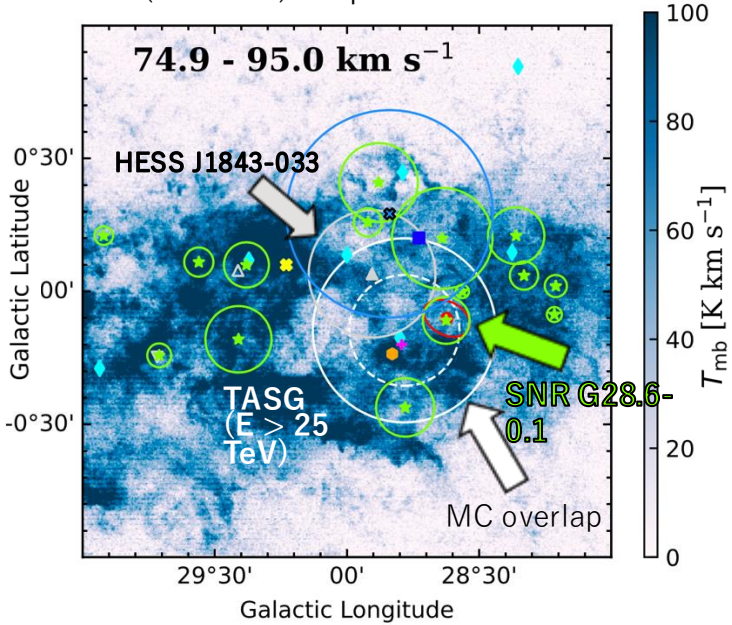

Several resemblances to SNR G106.3+2.7[2)]:

1. Overlapping molecular clouds (MCs),
2. Max. energy of CR protons: ≃ 500TeV, &
3. Average of the estimated ages is ≃ 10 kyr.

=> **Could have been a PeVatron in the past??**

Diffusion time of CR protons through MCs[3)]:

$$\tau_{\rm diff} = \frac{R_{\rm cl}^2}{6D(E)} \sim 1.2\cdot 10^4 \chi^{-1} \left(\frac{R_{\rm tot}}{20\ {\rm pc}}\right)^2 \left(\frac{E}{\rm GeV}\right)^{-0.5} \left(\frac{B}{10\ \mu{\rm G}}\right)^{0.5} {\rm yr}$$

where R, size of MCs & χ , suppression factor.
Assuming χ = 0.1 & B = 10 μ G ($n_H \sim 100$ cm^{-3}),

$\tau_{\rm diff}(R_{\rm TASG}, E_{\rm CR} > 250\ {\rm TeV}) \lesssim 2.0\ {\rm kyr}$ &

$\tau_{\rm diff}(R_{\rm HESS}, E_{\rm CR} \simeq 10\ {\rm TeV}) \simeq 4.9\ {\rm kyr}.$

Acceptable compared w/ the SNR's age

1) Umemoto et al., PASJ 69, 78 (2017)
2) Amenomori et al., Nat. Astron. 5, 460 (2021)
3) Gabici et al., Astrophys. Space Sci. 309, 365 (2007)

Amenomori et al., ApJ 932, 120 (2022)

TASG J1844-038

Discussion (2): Association of TASG J1844-038 w/ PSR J1844-0346

PSR J1844-0346

- Gamma-ray PSR discovered by the Einstein@home project[1)]
- P = 113 ms, τ_c = 12 kyr & $\dot{E} = 4.2 \times 10^{36}$ erg s^{-1}
- Pseudo distance: 4.3 kpc[2)]

HESS J1843-033[3)]

- L (1 TeV < E < 10 TeV) = 2.4×10^{34} erg s^{-1} [3)] (@ 4.3 kpc)
- Size: ≃ 18 pc (@ 4.3 kpc)
- Spectral index: ≃ 2.0 (from the ECPL fit in this work)

=> has characteristics typical of TeV PWNe[4)].

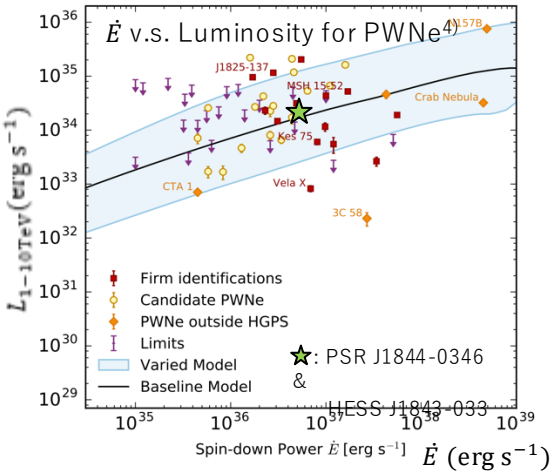

ICS off CMB is acceptable

- $e^{\pm}$ w/ E ≈ 90 TeV scatters off CMB up to $E_{\gamma,\,\mathrm{cutoff}} \approx 50$ TeV[5)].
- Size of TASG J1844-038: ≃ 26 pc (@ 4.3 kpc)
- Assuming Geminga-like env.[6)] with B = 3 μG, D = 4.4×10^{27} cm^2 s^{-1}, $\tau_{\mathrm{diff}} \simeq 8$ kyr
- Cooling time of $e^{\pm}$ by sync. & ISC[5)]: $\tau_{\mathrm{cool}} \simeq 11$ kyr

=> $\tau_{\mathrm{diff}} < \tau_{\mathrm{cool}}$ & $\tau_{\mathrm{diff}} < \tau_c$

1) Clark et al., ApJ 834, 106 (2017)
2) Devin et al., A&A 647, 68 (2021)
3) H.E.S.S. collaboration, A&A 612, A1 (2018)
4) H.E.S.S. collaboration, A&A 612, A2 (2018)
5) Hinton & Hofmann, Ann. Rev. of Astron. & Astrophys. 47, 523 (2009)
6) Abeysekara et al., Science 358, 911 (2017b)

Moon Shadow as a Calibration Source

- ✓Absolute Energy Scale
  - Energy dependence of E-W displacement
- ✓Pointing Accuracy
  - N-S displacement
- ✓Angular Resolution
  - Deficit Shape
- ✓Detector Stability
  - Temporal variation
- ✓Anti-P / P Ratio
  - Opposite-side deficit

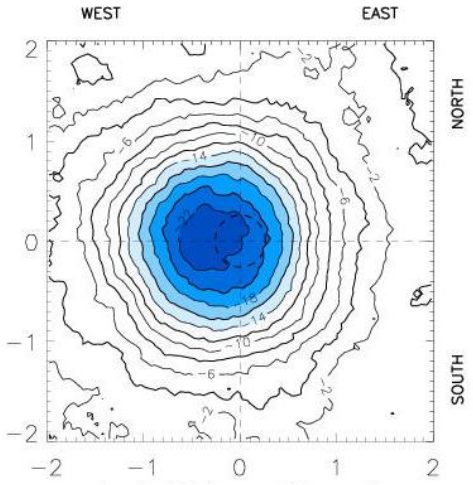

$$\Delta\theta \sim \frac{1.6^o}{E[\mathrm{TeV}]}$$

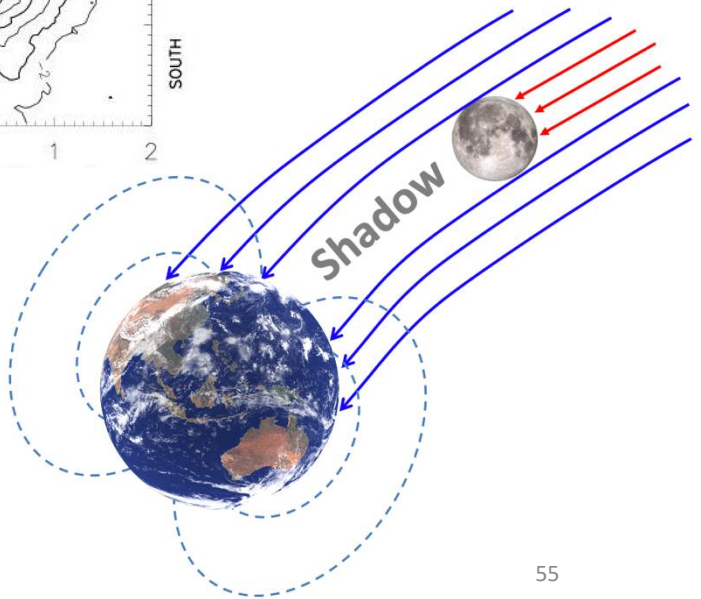

Moon Shadow as a Calibration Source

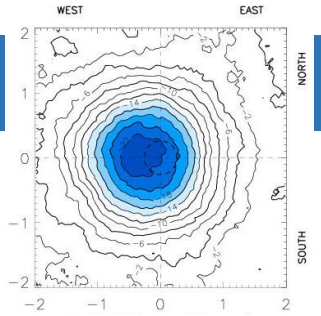

✓ Tibet ASγ experiment first time utilized the Moon shadow as the absolute energy calibration.

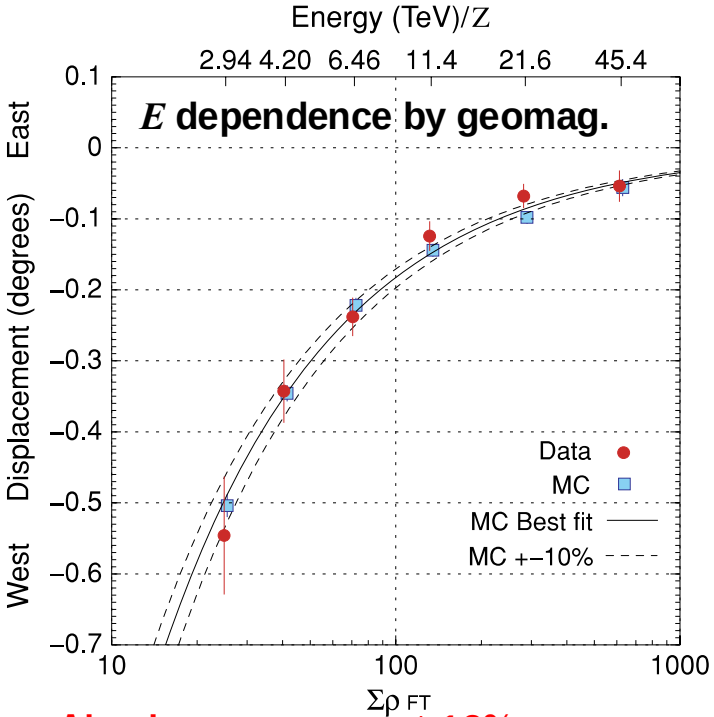

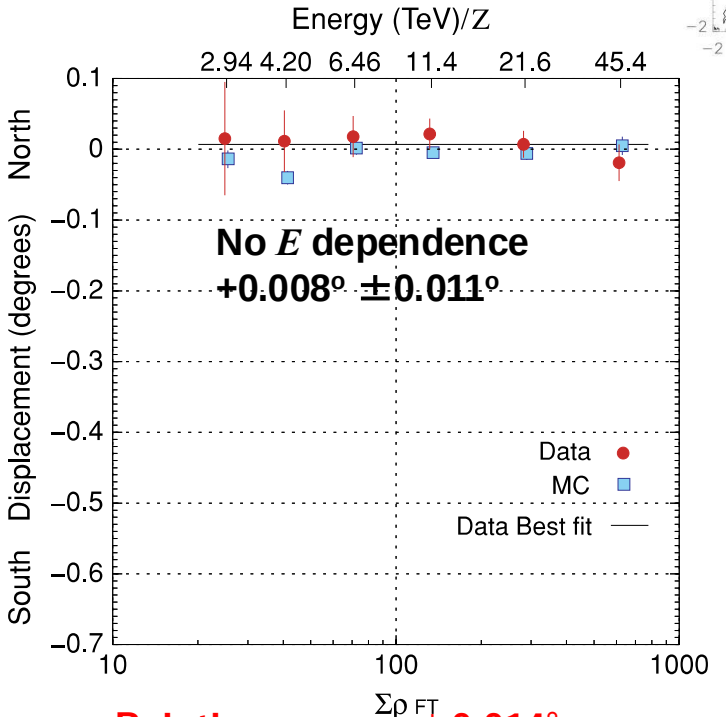

Absolute E error = ±12%

Best-fit = -4.5%(±8.6stat.±6.7sys.)%

Pointing error = ±0.014°

Amenomori et al., ApJ (2009), ICRC2005

Crab Nebula

Amenomori et al., PRL 123, 051101 (2019)

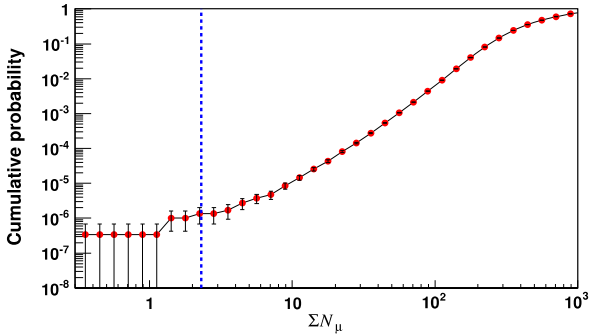

FIG. 4. Cumulative probability (P_μ) of ΣN_μ for cosmic-ray events above 251 TeV, which are recorded under similar geometries ($\theta \pm 5°$ and $r_{\rm core} \pm 30$ m) as the 251 TeV photonlike event in Fig. 1. The vertical dashed line indicates $\Sigma N_\mu = 2.3$ detected in the 251 TeV photonlike event.

TABLE I. Probability of misidentifying cosmic-ray events from the Crab as a photonlike event ($P_{\rm CR}$) for each of four photonlike events above 250 TeV together with other reconstructed values. θ and $r_{\rm core}$ are the zenith angle and core distance from the AS array center, respectively.

E (TeV)	ΔE (TeV)	$\Sigma\rho$	ΣN_μ	θ (°)	$r_{\rm core}$ (m)	ϕ^2 (deg^2)	$P_{\rm CR}(>E)$
251	$^{+46}_{-43}$	3248	2.3	29.8	35.1	0.00	1.7×10^{-3}
313	$^{+58}_{-54}$	2440	5.5	27.5	94.6	0.03	2.2×10^{-2}
449	$^{+112}_{-97}$	2307	11.3	35.4	93.3	0.12	2.9×10^{-2}
458	$^{+83}_{-78}$	2211	21.5	27.5	111.6	0.18	0.23

Source Contribution to the Tibet GDE Flux @ ＞100TeV

10^{-4} $25° < l < 100°, |b| < 5°$

Sub-PeV 1LHAASO sources & Tibet GDE masked regions

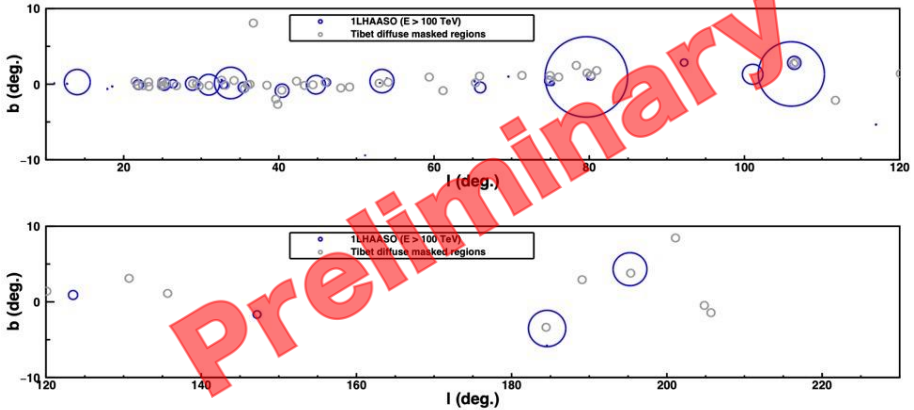

Tibet masked regions should be considered
to properly account for the source contribution

LHAASO GDE masked regions
(15°＜l＜125°)

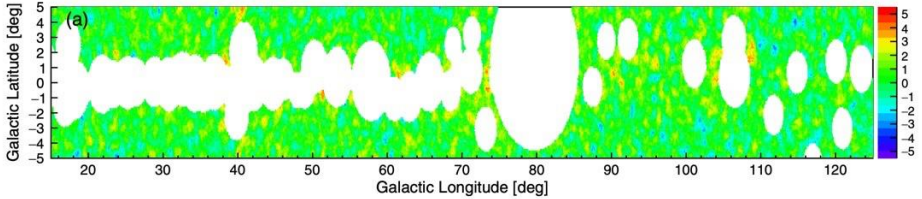

LHAASO masked region should be considered
to discuss Tibet GDE / LHAASO GDE ~ 5

Questions:
Significant contribution to Tibet GDE from LHAASO src.s?
Tibet GDE / LHAASO GDE ~ 5 @ 100TeV. How to explain it?

Nature of the Tibet GDE Flux

IceCube Collaboration, Science 380, 1338 (2023)

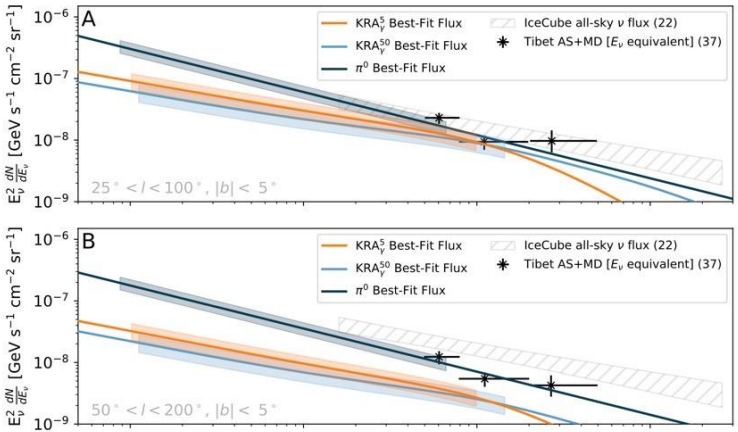

Fang & Murase, ApJL 957, L6 (2023)

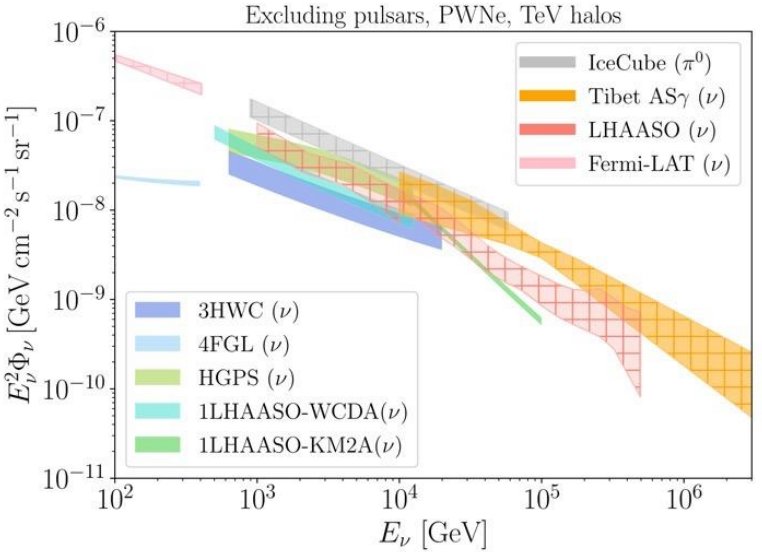

Consistent w/ IC ν flux (π^0 model)
=> Supporting the hadronic origin of Tibet GDE

IC ν flux (π^0 model) is likely dominated by diffuse emission
=> Supporting the diffusive nature of Tibet GDE

=> IC & LHAASO observation supports that Tibet GDE is truly of hadronic diffusive nature